รายงานการวิจัยฉบับสมบูรณ์

วงจรกระจายสัญญาณสำหรับเครือข่ายไร้สาย

Coupler Circuit for Wireless Application

ทุนวิจัยภายใต้บันทึกข้อตกลงความร่วมมือ รหัสโครงการ KREF156101

คณะผู้วิจัย

หัวหน้าโครงการ นายฉัตรพล ภคศิริ

ผู้ร่วมวิจัย นาย Sen Wang

นาย Nien-Sheng Yang

ได้รับการสนับสนุนเงินวิจัยจาก กองทุนวิจัย ประจำปี พ.ศ. 2561

วิทยาลัยนวัตกรรมการผลิตขั้นสูง

สถาบันเทคโนโลยีพระจอมเกล้าเจ้าคุณทหารลาดกระบัง

บทคัดย่อ

ในปัจจุบันอุปกรณ์ไร้สายได้เข้ามามีบทบาทในชีวิตประจำวัน วงจรสำหรับการส่งสัญญาณไร้สายจึงจำเป็นต้องมีการพัฒนาเพื่อเพิ่มประสิทธิภาพ ในวงจรด้านรับสัญญาณ วงจรกระจายสัญญาณเป็นวงจรสำคัญในการนำสัญญาณไปประมวลผลที่ภาครับ วงจรกระจายสัญญาณในโครงการนี้จะศึกษาวงจรกระจายสัญญาณแบบผลต่างที่สัญญาณเอาท์พุทสองพอร์ต และมีการลดระดับสัญญาณที่อีกเอาท์พุทพอร์ต หรือเรียกว่าวงจรแรทเรซ (rat-race coupler) ในการออกแบบวงจรจะออกแบบให้วงจรสามารถเชื่อมต่อกับวงจรภายนอกที่มีค่าอิมพีแดนซ์เป็นจำนวนเชิงซ้อนได้ วงจรที่ออกแบบจะอยู่ในรูปของแผ่นวงจร (printed circuit board) และวงจรรวม (integrated passive device chip) โดยวงจรในแผ่นวงจรจะทำงานได้ถึงสองย่านความถี่ ส่วนในรูปแบบวงจรรวมจะทำงานได้ที่หนึ่งย่านความถี่

คำสำคัญ : rat-race coupler, complex impedance termination, integrated passive device.

Research Title: Coupler Circuit for Wireless Application

Researcher: Chatrpol Pakasiri (King Mongkut's Institute of Technology Ladkrabang)

Faculty: College of Advanced Manufacturing Innovation

Researcher: Sen Wang (National Taipei University of Technology, Taiwan)

Researcher: Nien-Sheng Yang (National Taipei University of Technology, Taiwan)

ABSTRACT

At present, wireless devices play key role in modern society. Transmitter circuits performance need to be more and more efficient. Similarly, receiver circuits are also important and needed to be improved. In receivers, coupler circuits play key role in determining their performance since they are the very early part of the circuits in receiving data. In this project coupler circuits with differential output signals are studied. The circuit, called rat-race coupler, has four ports: one input port, two output ports and one isolation port. In connecting the coupler to other circuits, the impedance of other circuits maybe complex values. Therefore, the rat-race coupler must be able to be used with complex termination. The circuit are designed based on two platforms: one in printed circuit board (PCB) and the other in integrated passive device (IPD). The PCB type works with dual frequency bands while the IPD type works on single frequency of operation.

Keywords : rat-race coupler, complex impedance termination, integrated passive device.

กิตติกรรมประกาศ

คณะผู้วิจัยขอขอบคุณ National Chip Implementation Center (CIC) ที่ให้การสนับสนุนในการทำวงจรรวม การวิจัยครั้งนี้ได้รับทุนสนับสนุนการวิจัยจากสถาบันเทคโนโลยีพระจอมเกล้าเจ้าคุณทหารลาดกระบังผ่านทางทุนวิจัยภายใต้บันทึกข้อตกลงความร่วมมือ รหัสโครงการ KREF156101 และ จาก National Taipei University of Technology ผ่านทาง National Taipei University of Technology-King Mongkut's Institute of Technology Ladkrabang (NTUT-KMITL) Joint Research Program รหัสโครงการ NTUT-KMITL-106-02 ประจำปีงบประมาณ พ.ศ. 2561

ฉัตรพล ภคศิริ

Sen Wang

Nien-Sheng Yang

สารบัญ

หน้า

สารบัญตาราง

ตารางที่ **หน้า**

สารบัญภาพ

ภาพที่ **หน้า**

Chapter 1

Introduction

In wireless communication, low cost circuits are normally in high demand. Therefore, most of the systems are implemented on chip as integrated circuit. At present, CMOS (Complementary metal-oxide-semiconductor) is the most popular one due to its low cost. Nevertheless, for wireless communication circuit, high frequency operation is usually needed. In this regards, the CMOS process has a setback because inductors at high frequency are quite lossy when implemented on CMOS process. To overcome this problem, another chip which is passive device containing inductors and capacitors is made separately. Then these two chips are integrated in system in package (SIP) form. The passive device chip is normally referred to as "Integrated Passive Device", IPD. Its characteristics is described in chapter 2.

1.1 Problem background

In wireless receiving circuit, a coupler circuit is a critical block in receiving signal. Once the signal is received, the coupler circuit separates the signal into two parts and sends the signal to later blocks for process. The signal output of the coupler circuit must be in differential form. A coupler circuit that separates signal into two paths with four port termination is called rat-race coupler. The circuit consists of one input port, two differential output ports and one isolated port as shown in Fig. 1.1.

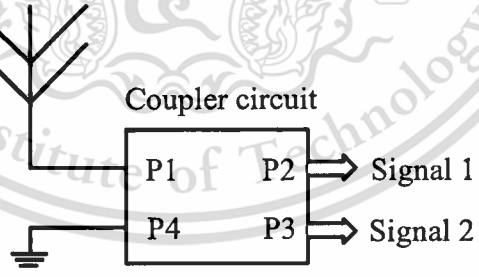

Fig.1.1 Receiving system.

To connect with other circuit blocks, the coupler output impedance at each port must be matched to the input impedance of the other blocks. The input impedance of the other blocks can be represented as termination impedance at each port. Conventional rat-race coupler has real termination impedance value. Nevertheless, in some cases, the input impedance of the other circuit blocks is complex impedance and therefore the termination impedances are complex

values. In this research, an identical complex impedance termination at all ports is used in the analysis and design.

Another research interest is the ability of the rat-race coupler circuit to be working in two different frequency bands. Since wireless devices nowadays works at various operating frequencies, a rat-race coupler circuit with multiple operating frequencies is desirable. In this research, a dual band rat-race coupler circuit with complex termination is also studied.

1.2 Research Purpose

To design a rat-race coupler circuit that can work with complex termination and operates in single or double frequency bands.

1.3 Research Scope

Two rat-race coupler circuit protobypes work in single and dual- frequency band of operation.

1.4 Methodology

The rat-race coupler circuit with complex termination is first analyzed by using distributed transmission lines. Then the transmission line components are replaced by lumped component circuits to reduce the size of the circuit. In the implementation, two forms are considered. One is on printed circuit board (PCB). The other is in Integrated Passive Device Process (IPD).

For the PCB prototype, the design starts with designing distributed transmission lines. Then all distributed transmission lines are replace with lumped component circuit. There are some concerns in implementation on PCB. Because layout traces on PCB are made of copper and have some length, these traces can cause errors in the design. To reduce the errors, layout traces can be represented by parasitic lump components. Electromagnetic simulation program is used to extract these parasitics. In the design, these parasitics are used together with lumped components. Therefore, the lumped components used have different value from ideal lumped component. Then there are two simulation results, e.g., one uses ideal lumped component values, the other uses layout parasitics with lumped components. The simulation with layout parasitics is referred to as 'post-simulations'.

For IPD process, the design also starts with designing all distributed transmission lines. Then all the distributed transmission lines are replaced with lumped components. To implement lumped components, parallel plate capacitors and rectangular spiral inductors are used. Each component is designed by using electromagnetic simulation program. When they are combined with layout, they must be adjusted to accommodate parasitics from the layout as well.

1.5 Research Benefits

The rat-race circuit can be most receiver circuits and the design technique can be applied to be used in other applications as well.

This report organizes as follows: chapter 2 introduces complex termination rat-race coupler on PCB, chapter 3 shows analysis and design of complex termination rat-race coupler on IPD process and finally chapter 4 draws conclusions.

Chapter 2

A Compact UHF Dual-Band Rat-Race Coupler with Complex Impedance Load

Rat-race coupler circuits are used in many circuit blocks such as low noise amplifier, power splitter, etc. The circuits have been implemented in many forms, e.g., on printed-circuit board (PCB), on CMOS platform or on Integrated Passive Device (IPD) platform. On PCB, the circuits have been studied in distributed types [1-3] and lumped component types [4-6]. A combination of distributed and lumped component types are reported in [7]. Each platform provides different advantages over various applications. Each platform provides different advantages over various applications. For lumped components types, the circuit size can be made smaller compared with distributed types.

Most of the times, rat-race circuit needs to be integrated with other circuits. Therefore, the terminated loads are usually complex impedance loads. The requirement for rat-race circuits to work with complex impedance loads is of great benefits. In 2013, Q. He, et al. [3] proposed novel 180 ° rat-race hybrid with arbitrary power division for complex impedances. The circuit operates at single frequency with all ports terminated with identical complex loads. The signals at two output ports are equal in magnitude and in phase while that of the other output port is null. In this paper, a compact dual-band rat-race coupler with complex impedance loads is proposed. The example circuits works at 450/900 MHz with output signals being out of phase. The proposed theory of the circuit is based on transmission lines, and the circuit is transformed to lumped components for further size reduction.

2.1 DUAL-BAND RAT-RACE COUPLER WITH COMPLEX IMPEDANCE TERMINAL LOAD

In this section, the dual-band rat-race coupler with complex load is designed and analyzed by using transmission lines. Properties of the three TLs in the circuit are identified. Then all three transmission lines are transformed to lumped component circuits. The transformation equations to two type of lumped circuits are given.

2.1.1. Dual-band rat-race coupler design with transmission lines

Figure 2.1 shows the proposed dual-band rat-race coupler, and all four ports are terminated with the same complex load value of Z_L. The load impedance values at the first and second operating frequency are defined as $Z_{L1}=R_{L1}+jX_{L1}$ and $Z_{L2}=R_{L2}+jX_{L2}$, respectively. The first

TL has characteristic impedance Z_1 with electrical length $2\theta_1$ at the frequency of interest. Similarly, the second TL has characteristic impedance Z_2 with electrical length θ_2, and the third TL features characteristic impedance Z_3 with electrical length $2\theta_3$. The circuit properties are defined as follows.

$$S_{11}=0 \tag{2.1}$$

$$|S_{21}|=|S_{31}| \tag{2.2}$$

$$\angle S_{21}-\angle S_{31}=\pm 180^{\circ} \tag{2.3}$$

$$S_{41}=0 \tag{2.4}$$

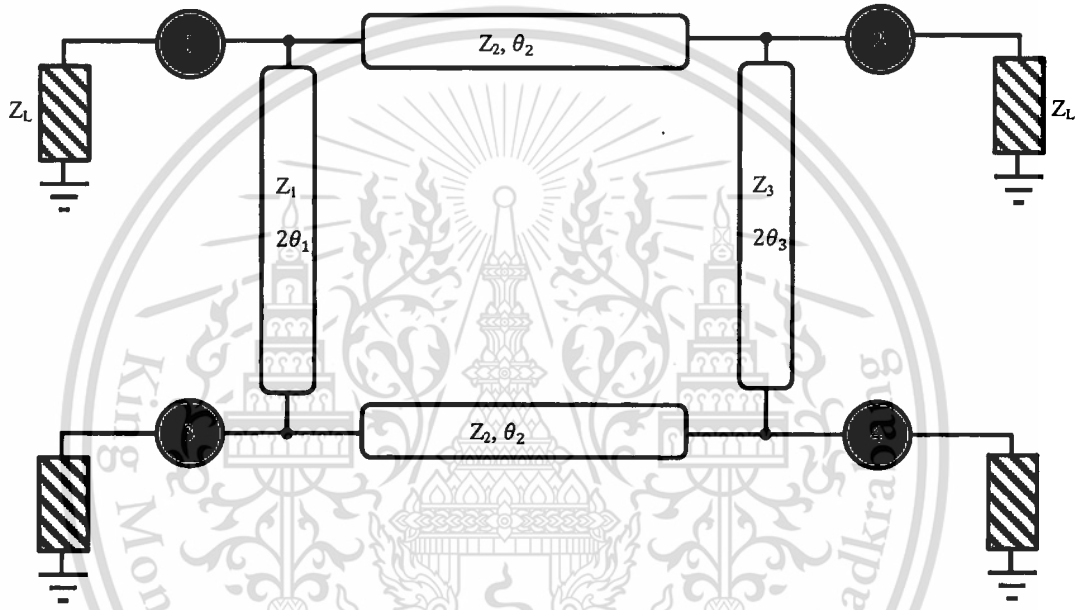

Fig. 2.1 The proposed rat-race coupler with complex load termination, Z_L.

By applying even and odd mode analysis, the circuit can be replaced by half-circuits as shown in Fig. 2.2.

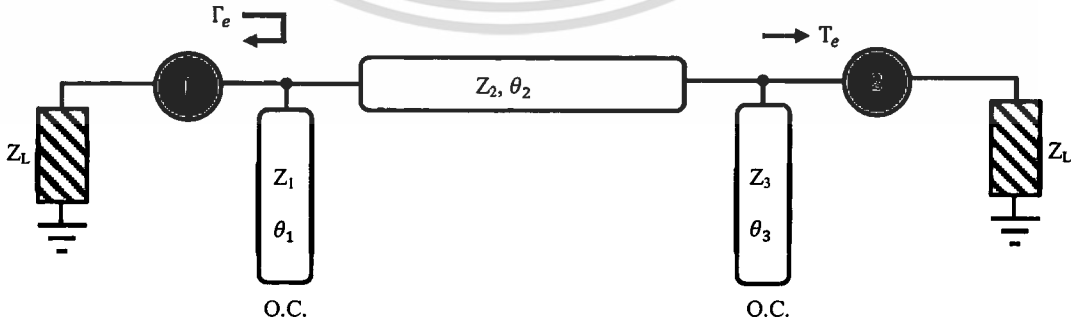

(a)

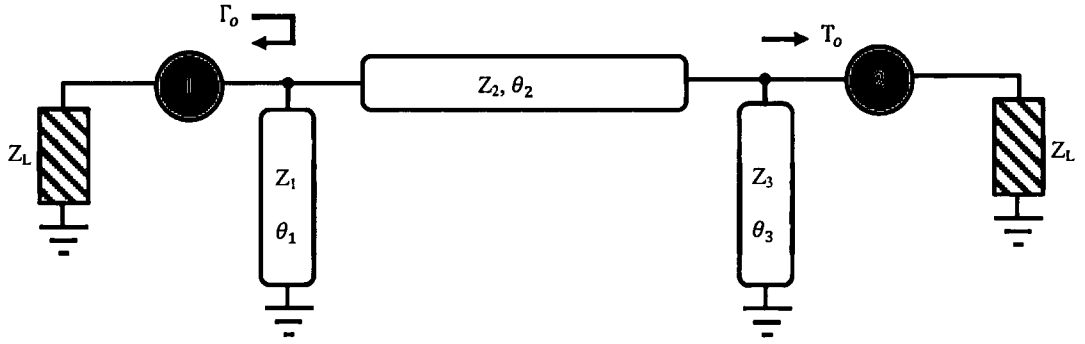

(b)

Fig. 2.2 Equivalent circuit for (a) even- and (b) odd- mode analysis.

The $[ABCD]_e$ matrix of the even mode can be calculated as

$$A_e = \cos(\theta_2) - \frac{Z_2 \sin(\theta_2)\tan(\theta_3)}{Z_3}, \tag{2.5a}$$

$$B_e = jZ_2 \sin(\theta_2), \tag{2.5b}$$

$$C_e = j[\frac{\cos(\theta_2)\tan(\theta_1)}{Z_1} + \frac{\sin(\theta_2)}{Z_2} - \frac{jZ_2 \sin(\theta_2)\tan(\theta_1)\tan(\theta_3)}{Z_1 Z_3} + \frac{\cos(\theta_2)\tan(\theta_3)}{Z_3}], \tag{2.5c}$$

$$D_e = \frac{-Z_2}{Z_1}\sin(\theta_2)\tan(\theta_1) + \cos(\theta_2). \tag{2.5d}$$

Similarly, the $[ABCD]_o$ matrix of the odd mode can be calculated as

$$A_o = \cos(\theta_2) - \frac{Z_2 \sin(\theta_2)}{Z_3 \tan(\theta_3)}, \tag{2.6a}$$

$$B_o = jZ_2 \sin(\theta_2), \tag{2.6b}$$

$$C_o = j[\frac{-\cos(\theta_2)}{Z_1 \tan(\theta_1)} + \frac{\sin(\theta_2)}{Z_2} - \frac{jZ_2 \sin(\theta_2)}{Z_1 Z_3 \tan(\theta_1)\tan(\theta_3)} - \frac{\cos(\theta_2)}{Z_3 \tan(\theta_3)}], \tag{2.6c}$$

$$D_o = \frac{Z_2 \sin(\theta_2)}{Z_1 \tan(\theta_1)} + \cos(\theta_2). \tag{2.6d}$$

From the $[ABCD]$ matrix, the reflection and transmission coefficients of both even and odd modes can be written as

$$\Gamma_e = \frac{A_e Z_L + B_e - C_e |Z_L|^2 - D_e Z_L^*}{A_e Z_L + B_e + C_e Z_L^2 + D_e Z_L}, \tag{2.7a}$$

$$\Gamma_o = \frac{A_o Z_L + B_o - C_o |Z_L|^2 - D_o Z_L^*}{A_o Z_L + B_o + C_o Z_L^2 + D_o Z_L}, \tag{2.7b}$$

$$\mathrm{T}_e = \frac{2\,\mathrm{Re}(Z_L)}{A_e Z_L + B_e + C_e Z_L^2 + D_e Z_L}, \tag{2.7c}$$

$$T_o = \frac{2\,\mathrm{Re}(Z_L)}{A_o Z_L + B_o + C_o Z_L^2 + D_o Z_L}. \tag{2.7d}$$

Then desired S-parameters of the circuit are

$$S_{11} = \frac{1}{2}(\Gamma_e + \Gamma_o), \tag{2.8a}$$

$$S_{21} = \frac{1}{2}(T_e + T_o), \tag{2.8b}$$

$$S_{31} = \frac{1}{2}(\Gamma_e - \Gamma_o), \tag{2.8c}$$

$$S_{41} = \frac{1}{2}(T_e - T_o). \tag{2.8d}$$

The relationships between S-parameters in equations (8) and ABCD-parameters in equation (5)-(7) were calculated in [1]. It was found in [1] that the relationships between the first and third transmission line are

$$Z_1 = Z_3 = m, \tag{2.9}$$

$$\theta_3 = \theta_1 + \frac{\pi}{2} + n\pi. \tag{2.10}$$

Therefore, the unknown parameters for rat-race circuit are reduced to four unknowns $(m, \theta_1, Z_2, \theta_2)$ for each operating frequency. To achieve the rat-race circuit conditions in (1)-(4), four equations for must be satisfied as follows:

$$Z_2 \sin(\theta_2) = -m \cdot \sin(2\theta_1), \tag{2.11}$$

$$[\cos(\theta_2) - \frac{Z_2}{m}\sin(\theta_2)\tan(\theta_1 + \frac{\pi}{2})]X_{L1} + Z_2 \sin(\theta_2) - [\frac{\cos(\theta_2)\tan(\theta_1)}{m} + \frac{\sin(\theta_2)}{Z_2}$$

$$-\frac{Z_2}{m^2}\sin(\theta_2)\tan(\theta_1)\tan(\theta_1 + \frac{\pi}{2}) + \frac{\cos(\theta_2)\tan(\theta_1 + \frac{\pi}{2})}{m}](R_{L1}^2 + X_{L1}^2) \quad , \tag{2.12}$$

$$+[-\frac{Z_2}{m^2}\sin(\theta_2)\tan(\theta_1) + \cos(\theta_2)]X_{L1} = 0$$

$$Z_2 \sin(k \cdot \theta_2) = -m \cdot \sin(k \cdot 2\theta_1), \tag{2.13}$$

$$[\cos(k \cdot \theta_2) - \frac{Z_2}{m}\sin(k \cdot \theta_2)\tan(k \cdot \theta_1 + \frac{\pi}{2})]X_{L1} + Z_2 \sin(k \cdot \theta_2) - [\frac{\cos(k \cdot \theta_2)\tan(k \cdot \theta_1)}{m}$$

$$+\frac{\sin(k \cdot \theta_2)}{Z_2} - \frac{Z_2}{m^2}\sin(k \cdot \theta_2)\tan(k \cdot \theta_1)\tan(k \cdot \theta_1 + \frac{\pi}{2}) + \quad ,$$

$$\frac{\cos(k \cdot \theta_2)\tan(k \cdot \theta_1 + \frac{\pi}{2})}{m}](R_{L1}^2 + X_{L1}^2) + [-\frac{Z_2}{m^2}\sin(k \cdot \theta_2)\tan(k \cdot \theta_1) + \cos(k \cdot \theta_2)]X_{L1} = 0$$

(2.14)

where k is the ratio of the second to the first operating frequency, $k=f_2/f_1$. For dual-band operation, all TLs except TL_3 calculated from (11)-(14) can be realized using conventional microstrip lines. Because of the requirement in (10), a conventional microstrip line cannot satisfy the electrical length requirement of both operating frequencies for TL_3. To solve this problem, lumped circuits are used to replace the TLs. The dual-band and distributed-lumped element transformation will be detailed in the next section.

2.1.2. Dual-band rat-race coupler design with lumped components

Consider a transmission line with Z_0 characteristic impedance. The transmission line has θ_{f1} electrical length at the first operating frequency and θ_{f2} electrical length at the second operating frequency. To replace a microstrip line with lumped components, two types of circuits are used which are band-pass and band-stop circuit topologies. Figure 2.3 shows the lumped circuit transmission line topologies. For the band-pass topology, the lumped components are related to the transmission line properties as

$$C_1 = \frac{\frac{\omega_1}{Z_o}(\csc(\theta_{f1}) - \cot(\theta_{f1})) - \frac{\omega_2}{Z_o}(\csc(\theta_{f2}) - \cot(\theta_{f2}))}{\omega_1^2 - \omega_2^2}, \tag{2.15a}$$

$$L_1 = \frac{\frac{1}{\omega_2^2} - \frac{1}{\omega_1^2}}{\frac{1}{Z_o\omega_1}(\csc(\theta_{f1}) - \cot(\theta_{f1})) - \frac{1}{Z_o\omega_2}(\csc(\theta_{f2}) - \cot(\theta_{f2}))}, \tag{2.15b}$$

$$C_2 = \frac{\frac{1}{\omega_2^2} - \frac{1}{\omega_1^2}}{\frac{1}{\omega_1}(\frac{2}{B_1} - \frac{\sin(\theta_{f1})}{Z_o B_1^2}) - \frac{1}{\omega_2}(\frac{2}{B_2} - \frac{\sin(\theta_{f2})}{Z_o B_2^2})}, \tag{2.15c}$$

$$L_2 = \frac{\omega_1(\frac{2}{B_1} - \frac{\sin(\theta_{f1})}{Z_o B_1^2}) - \omega_2(\frac{2}{B_2} - \frac{\sin(\theta_{f2})}{Z_o B_2^2})}{\omega_1^2 - \omega_2^2}, \tag{2.15d}$$

where ω_1 and ω_2 are angular frequencies at the first and second operating frequencies, respectively. The susceptance (B_1) at the first frequency and the susceptance (B_2) at the second frequency are related to the transmission line properties as

$$B_1 = \frac{1}{Z_o}(\csc(\theta_{f1}) - \cot(\theta_{f1})), \tag{2.16a}$$

$$B_2 = \frac{1}{Z_o}(\csc(\theta_{f2}) - \cot(\theta_{f2})). \tag{2.16b}$$

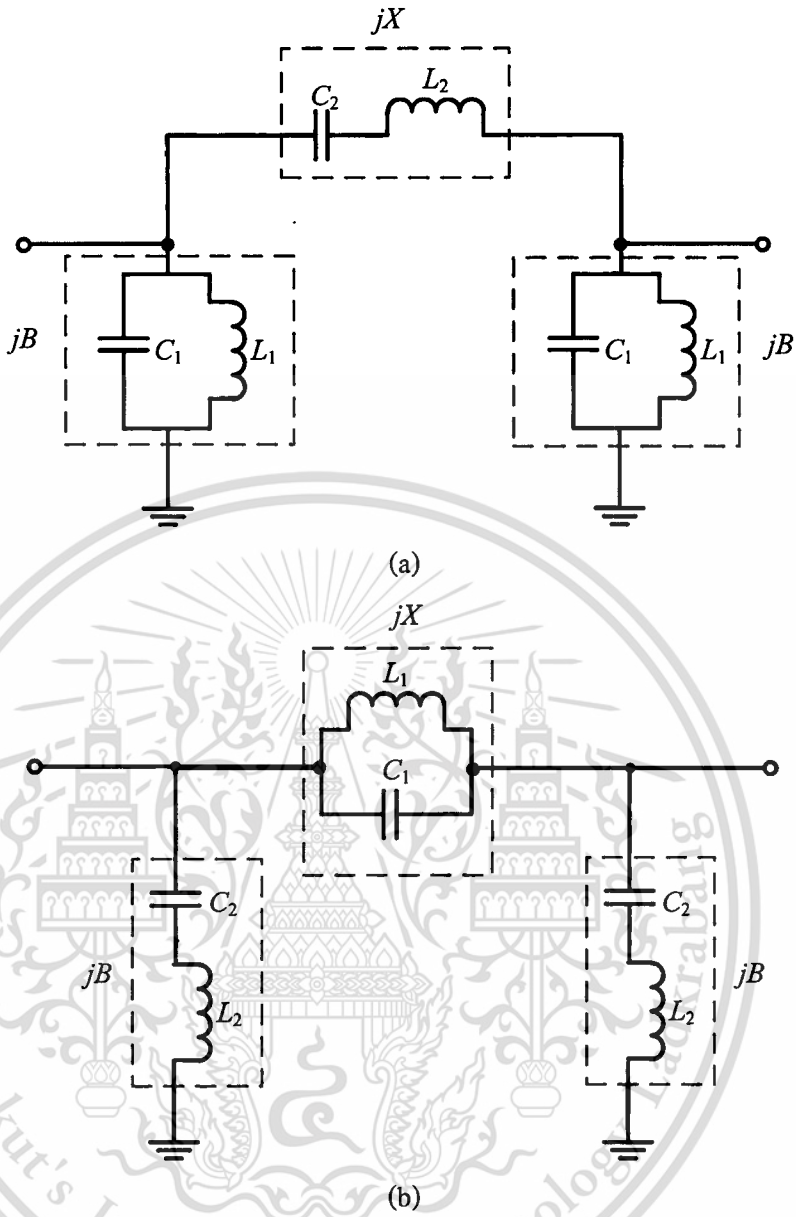

Fig. 2.3. (a) Band-pass circuit and (b) band-stop circuit topologies of a T.L.

For the band-stop topology, the lumped components are related to the transmission line properties as

$$C_1 = \frac{1}{\omega_2^2 - \omega_1^2}\left[\frac{\omega_1}{\left(\frac{2}{B_1} - \frac{\sin(\theta_{f1})}{Z_o B_1^2}\right)} - \frac{\omega_2}{\left(\frac{2}{B_2} - \frac{\sin(\theta_{f2})}{Z_o B_2^2}\right)}\right], \tag{2.17a}$$

$$L_1 = \frac{\frac{1}{\omega_1^2} - \frac{1}{\omega_2^2}}{\frac{1/\omega_1}{\left(\frac{2}{B_1} - \frac{\sin(\theta_{f1})}{Z_o B_1^2}\right)} - \frac{1/\omega_2}{\left(\frac{2}{B_2} - \frac{\sin(\theta_{f2})}{Z_o B_2^2}\right)}}, \tag{2.17b}$$

$$C_2 = \frac{\frac{1}{\omega_1^2} - \frac{1}{\omega_2^2}}{\frac{Z_o/\omega_1}{\csc(\theta_{f1}) - \cot(\theta_{f1})} - \frac{Z_o/\omega_2}{\csc(\theta_{f2}) - \cot(\theta_{f2})}}, \tag{2.17c}$$

$$L_2 = \frac{\frac{\omega_1 Z_o}{\csc(\theta_{f1}) - \cot(\theta_{f1})} - \frac{\omega_2 Z_o}{\csc(\theta_{f2}) - \cot(\theta_{f2})}}{\omega_2^2 - \omega_1^2}. \tag{2.17d}$$

In the next section, all three transmission lines in the rat-race circuit are designed with lumped components. The dual-band rat-race coupler operates at 450 MHz and 900 MHz.

2.2. IMPLEMENTATION AND MEASUREMENTS

An example circuit is designed with a complex impedance load. The rat-race circuit is designed to operate at 450 MHz (f_1) and 900 MHz (f_2). To implement a complex terminal at the rat-race port, a transformation circuit consisting of L-C ladder network shown in Fig. 2.4 is used. The source impedance is assumed to be 50 Ω. The load values at both operating frequencies are calculated to be $Z_L(f_1)$=33.11−j29.04 Ω and $Z_L(f_2)$=38.65−j4.65 Ω.

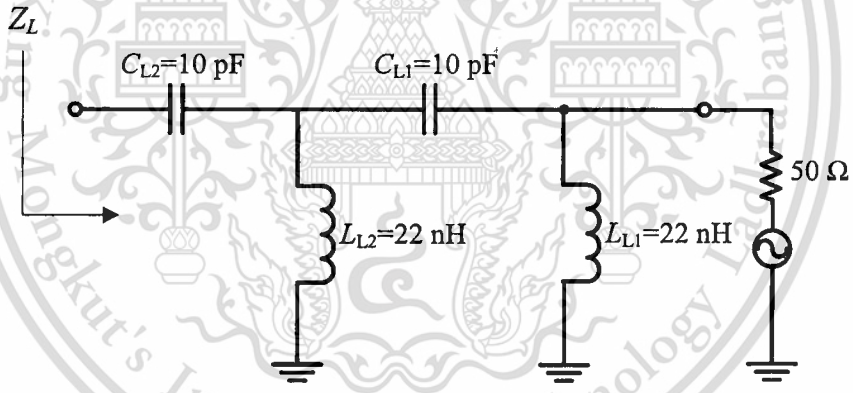

Fig. 2.4. Load transformation network.

Using the design equations (9)-(14), the properties of all three TLs are tabulated in Table 2.1. Then applying equations (15)-(17), ideal lumped components values are also shown in Table 2.2 as theoretical circuit. The circuits are implemented on a printed-circuit board (PCB) from Rogers Corporation, RO3010 having relative dielectric constant (ε_r) of 10.2 and loss tangent of 0.0022. The board thickness is 1.27 mm. To incorporate the PCB traces in the circuit, the layout of the circuit are simulated by Momentum in Advanced Design System (ADS). Then all lumped components are adjusted accordingly. The results are also shown in Table 2.2 as post-simulation circuit. In addition, the implemented circuit shown in the table uses practical lumped components for experiment. The prototype unit is shown in Fig. 2.5. The circuit size is 2.5×3.4cm^2, which is $0.075\lambda_2 \times 0.102\lambda_2$ where λ_2 is wavelength at 900 MHz.

Table 2.1. Transmission line properties for rat-race coupler with complex load Z_L.

Frequency (MHz)	Transmission line 1		Transmission line 2		Transmission line 3	
450	$Z_1 = 69.43\ \Omega$	$2\theta_1 = 243°$	$Z_2 = 69.43\ \Omega$	$\theta_2 = 243°$	$Z_3 = 69.43\ \Omega$	$2\theta_3 = 64°$
900	$Z_1 = 69.43\ \Omega$	$2\theta_1 = 127°$	$Z_2 = 69.43\ \Omega$	$\theta_2 = 127°$	$Z_3 = 69.43\ \Omega$	$2\theta_3 = 307°$

Table 2.2. Lumped component values of the transmission line sections

Component / Circuit #	Transmission line section	C_1 (pF)	L_1 (nH)	C_2 (pF)	L_2 (nH)
Theoretical Circuit	1	9.62	7.024	2.95	20.3
	2	6.18	10.55	4.40	13.16
	3	6.18	10.55	1.48	46.38
Post-simulation Circuit	1	3.84	10.77	4.15	11.66
	2	6.09	8.768	1.87	14.41
	3	6.15	11.03	0.57	26.19
Implemented Circuit	1	3.9	10	3.9	12
	2	5.8	8.7	1.8	15
	3	5.6	11	0.5	28

Using complex ports shown in Fig. 2.4, the *S*-parameters of the rat-race circuits are shown in Fig. 2.6. Table 2.3 summarizes the circuit performance at 450 MHz and 900 MHz. From the table, the theoretical circuit shows excellent performance as it meets all conditions in (1)-(4). With the layout integrated into the circuit, the performance of the post-simulation circuit is dropped. For the prototype unit, the performance of implemented circuit is dropped further. The lower performance of the post-simulation from the implemented circuit is caused by both using practical lumped components and having parasitic loss in components, especially the inductors.

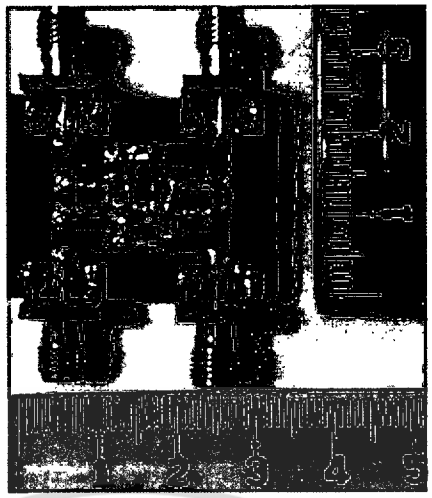

Fig. 2.5. Rat-race prototype photo.

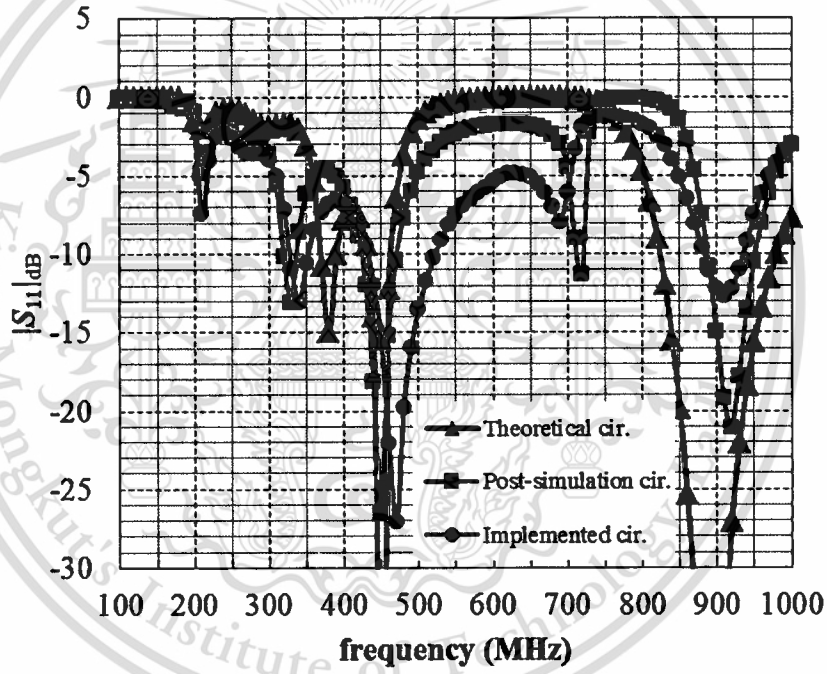

(a)

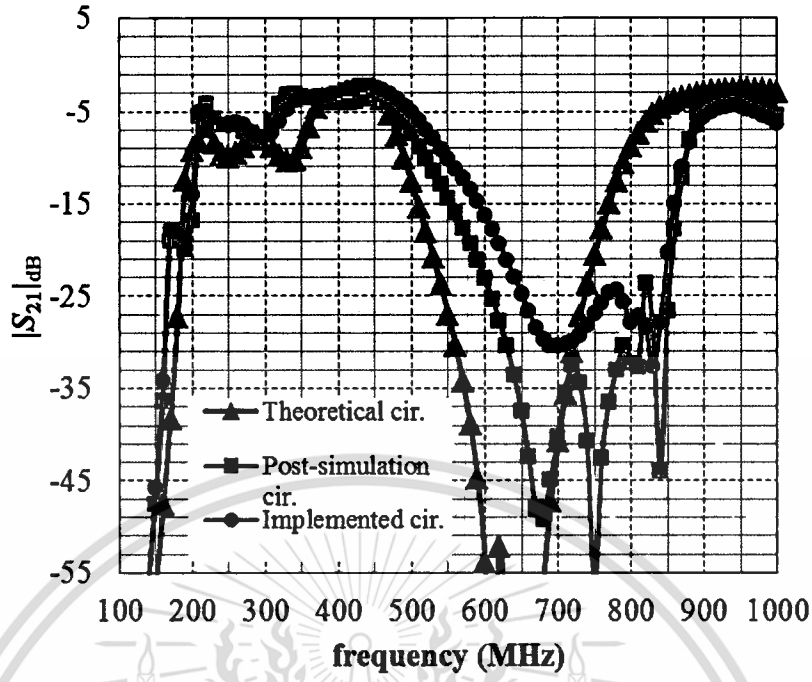

(b)

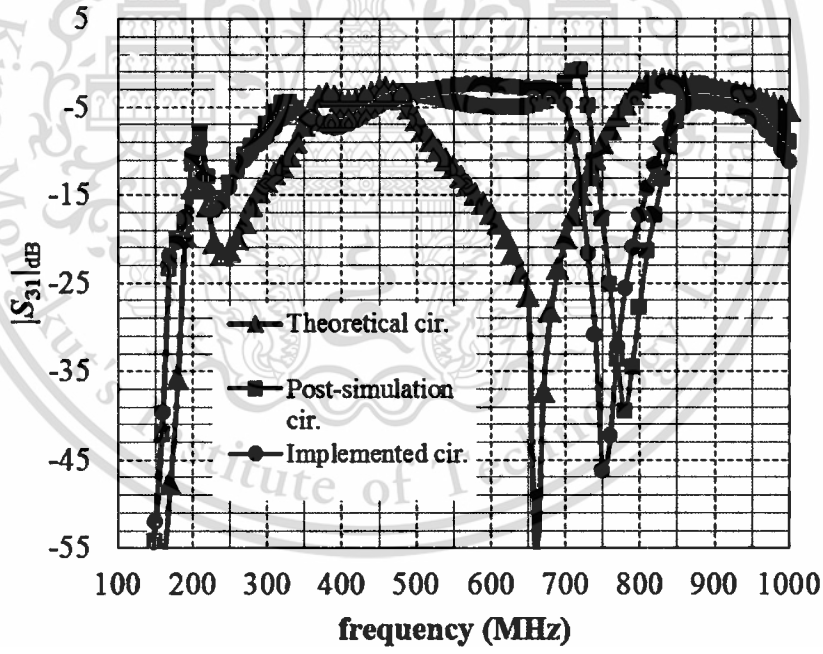

(c)

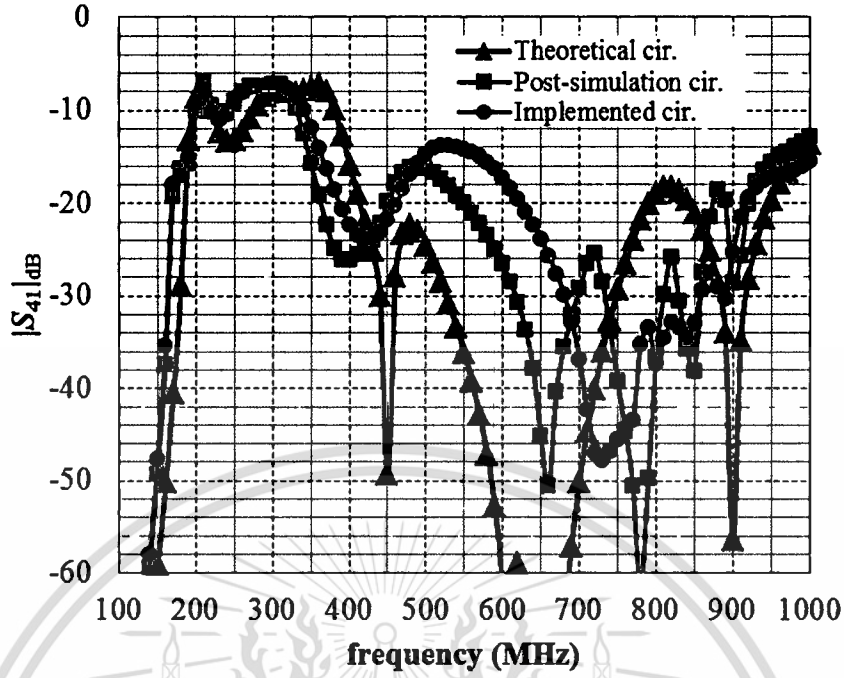

(d)

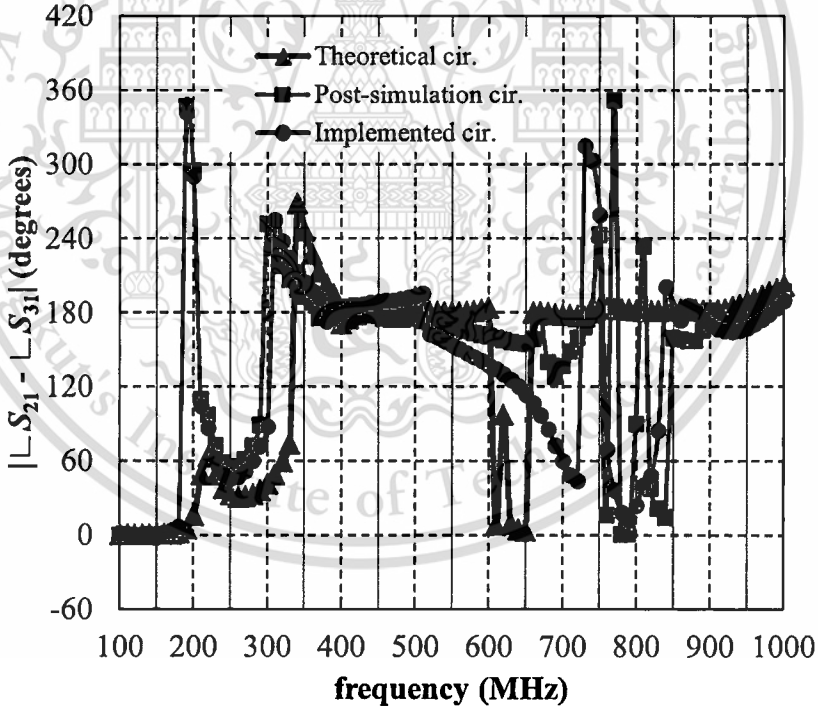

(e)

Fig. 2.6 *S*-parameters comparison of the rat-race circuits including (a) $|S_{11}|_{dB}$, (b) $|S_{21}|_{dB}$, (c) $|S_{31}|_{dB}$, (d) $|S_{41}|_{dB}$ and (e) $|\angle S_{21} - \angle S_{31}|$.

Table 2.3. Rat-race circuit performance

Frequency (MHz)	Conditions / Circuit #	$\lvert S_{11}\rvert_{dB}$	$\lvert S_{21}\rvert_{dB}$	$\lvert S_{31}\rvert_{dB}$	$\lvert S_{41}\rvert_{dB}$	$\lvert \angle S_{21} - \angle S_{31}\rvert$
450	Theoretical	-49	-3	-3	-49	180^0
	Post-simulation	-26	-2.6	-3.8	-20	183^0
	Implemented	-16	-2.4	-4.9	-22	188^0
900	Theoretical	-54	-3	-3	-56	180^0
	Post-simulation	-15	-3.8	-3	-15	181^0
	Implemented	-13	-5.6	-4.5	-25	170^0

2.3. CONCLUSIONS

In this chapter, a compact 450/900-MHz dual-band rat-race coupler with complex impedance load is designed, implemented, and measured. Lumped components are used to implement transmission line sections in the rat-race design for circuit miniaturization. The circuit simulation shows good performance at both frequencies. The measured circuit also shows good rat-race functions with slightly different performance from the simulation due to two factors: 1) using available lumped components to replace ideal values and 2) lossy lumped components, especially the losses in inductors. The proposed methodology is promising in design dual-band rat-race coupler with complex load termination.

Chapter 3

2.4 GHz Rat-Race Coupler with Complex Termination on IPD Process

Rat-race coupler are commonly used in microwave circuit. On printed-circuit board, the longest transmission line can be as long as $3\lambda/4$ for normal real termination load [1]. Many researches have been done to minimize the size of the circuit [2-5]. In CMOS process, the quality factor of inductors is usually small, and therefore the performance of circuits is degraded [2]. In LTTC process, performance of circuit is quite good because of availability of high quality factor of inductors. Nevertheless, the production cost of LTTC is relatively high. Integrated passive device (IPD) process becomes more popular because of its relatively low production cost. It also provides high quality factor for passive components and modules [6].

Complex termination is usually encountered in circuit design. In [7], a hybrid rat-race coupler with in phase output ports has been derived for complex termination. In this paper, a proposed rat-race coupler at ISM band is implemented on IPD process. The output port design is modified to have out-of-phase signals. The circuit ports are terminated with a complex impedance value. The input port is matched. There are one isolation port and two output ports with differential signal.

3.1. Rat-Race Coupler Circuit Properties

In this chapter, the rat-race circuit properties are defined as follows,

$$S_{11} = 0, \tag{3.1}$$

$$|S_{21}| = |S_{31}|, \tag{3.2}$$

$$\angle S_{21} - \angle S_{31} = \pm 180°, \tag{3.3}$$

$$S_{41} = 0, \tag{3.4}$$

where the input port is port 1, the output ports are port 2 and port 3 and the isolation port is port 4. Figure 3.1 shows the proposed rat-race structure. Each port is terminated with a complex impedance value, Z_L.

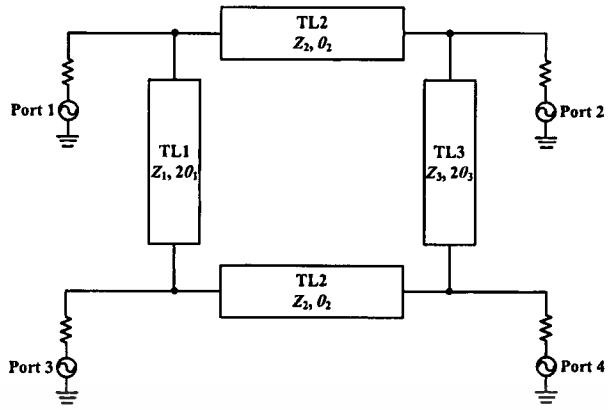

Fig. 3.1 The proposed rat-race coupler.

Because of the symmetric structure of the circuit, even and odd mode analysis can be applied. The analysis will be described next.

3.2. Even and Odd Mode Analysis

Figure 3.2 shows the structure when even mode is excited into the circuit. The first and the third transmission lines are separated in half, so does their electrical length. The reflection coefficient for the even mode can be found as

$$\Gamma_e = \frac{Z_{in}^{1e} - Z_L^*}{Z_{in}^{1e} + Z_L}, \tag{3.5a}$$

where

$$Z_{in}^{1e} = \frac{Z_{x2}^e(-jZ_1\cot(\theta_1))}{Z_{x2}^e + (-jZ_1\cot(\theta_1))}, \tag{3.5b}$$

$$Z_{x2}^e = Z_2\frac{Z_{x1}^e + jZ_2\tan(\theta_2)}{Z_2 + jZ_{x1}^e\tan(\theta_2)}, \tag{3.5c}$$

$$Z_{x1}^e = \frac{(-jZ_3\cot(\theta_3))Z_L}{(-jZ_3\cot(\theta_3)) + Z_L}. \tag{3.5d}$$

Note that * implies complex conjugate operator.

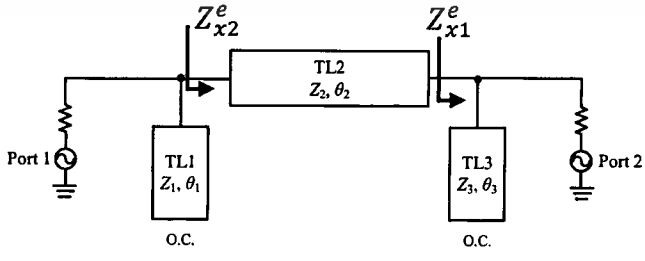

Fig. 3.2 Rat-race coupler for even mode analysis.

The transmission coefficient

$$T_e = \left(\frac{1+\Gamma_L^e}{e^{j\theta_2}+\Gamma_L^e e^{-j\theta_2}}\right)\left(\frac{Z_{ln}^{1e}}{Z_{in}^{1e}+Z_s}\right)\left(1+\frac{Z_L^*}{Z_L}\right), \tag{3.6a}$$

where

$$\Gamma_L^e = \frac{Z_{x1}^e - Z_2}{Z_{x1}^e + Z_2}. \tag{3.6b}$$

For the odd mode analysis, Fig. 3.3 shows the equivalent circuit. The reflection coefficient of the odd mode can be found as

$$\Gamma_o = \frac{Z_{in}^{1o} - Z_L^*}{Z_{in}^{1o} + Z_L}, \tag{3.7a}$$

where

$$Z_{in}^{1o} = \frac{Z_{x2}^o (jZ_1 \tan(\theta_1))}{Z_{x2}^o + (jZ_1 \tan(\theta_1))}, \tag{3.7b}$$

$$Z_{x2}^o = Z_2 \frac{Z_{x1}^o + jZ_2 \tan(\theta_2)}{Z_2 + jZ_{x1}^o \tan(\theta_2)}, \tag{3.7c}$$

$$Z_{x1}^o = \frac{(jZ_3 \tan(\theta_3))Z_L}{(jZ_3 \tan(\theta_3)) + Z_L}. \tag{3.7d}$$

The transmission coefficient for the odd mode is

$$T_o = \left(\frac{1+\Gamma_L^o}{e^{j\theta_2}+\Gamma_L^o e^{-j\theta_2}}\right)\left(\frac{Z_{ln}^{1o}}{Z_{in}^{1o}+Z_s}\right)\left(1+\frac{Z_L^*}{Z_L}\right), \tag{3.8a}$$

where

$$\Gamma_L^o = \frac{Z_{x1}^o - Z_2}{Z_{x1}^o + Z_2}. \tag{3.8b}$$

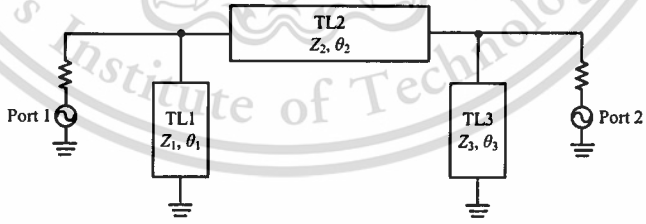

Fig. 3.3 Rat-race coupler for odd mode analysis.

Then S-parameters of the circuit can be found as

$$S_{11} = 0.5(\Gamma_e + \Gamma_o), \tag{3.9a}$$

$$S_{21} = 0.5(T_e + T_o), \tag{3.9b}$$

$$S_{31} = 0.5(\Gamma_e - \Gamma_o), \tag{3.9c}$$

$$S_{41} = 0.5(T_e - T_o). \tag{3.9d}$$

The relationships between the first and the third transmission line can be found as

$$Z_3 = Z_1, \tag{3.10}$$

$$\theta_3 = \theta_1 + \frac{\pi}{2} + n\pi. \tag{3.11}$$

The relationships between the first and the second transmission line can be found as

$$Z_2 \sin(\theta_2) = -Z_1 \sin(2\theta_1), \tag{3.12}$$

$$[\cos(\theta_2) - (Z_2/Z_1)\sin(\theta_2)\tan(\theta_1 + \pi/2)]X_{L1} + Z_2 \sin(\theta_2) - \left[\frac{\cos(\theta_2)\tan(\theta_2)}{Z_1} + \frac{\sin(\theta_2)}{Z_2} - \frac{Z_2}{Z_1^2}\sin(\theta_2)\tan(\theta_1)\tan\left(\theta_1 + \frac{\pi}{2}\right) + \frac{\cos(\theta_2)\tan\left(\theta_1 + \frac{\pi}{2}\right)}{Z_1}\right]|Z_L|^2 + \left[-\frac{Z_2}{Z_1^2}\sin(\theta_2)\tan(\theta_1) + \cos(\theta_2)\right]X_{L1} = 0, \tag{3.13}$$

where

$$Z_L = R_L + jX_L. \tag{3.14}$$

In the next section, a designed rat-race coupler on IPD process is discussed. The circuit layout is simulated by using ADS.

3.3. Rat-Race Coupler on IPD Process

The IPD process has three metal layers and two different types of dielectrics. The dielectric 1 and 2 have relative dielectric constant values of 6.7 and 2.65, respectively. The metal and via between the dielectric layers are made of copper. Figure 4 shows the cross section view of the IPD process.

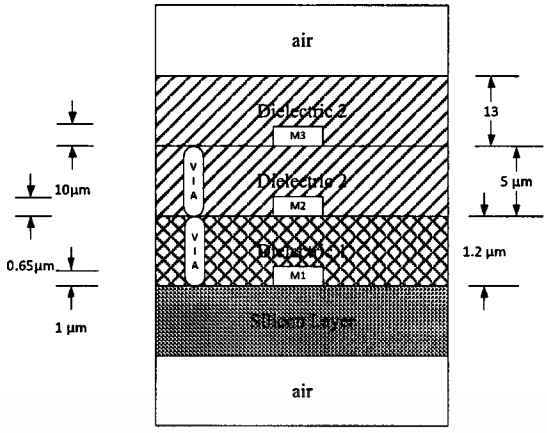

Fig. 3.4 Cross-section view of the IPD process.

An example circuit is set to have a complex terminal load value of $Z_L = 6.4 + j10\ \Omega$. Using design equations (10)-(13), all the transmission line properties are found and shown in Table 3.1.

Table 3.1 Transmission Line Properties of Rat-Race Circuit

Transmission Line	Characteristic Impedance (Ω)	Electrical Length (^{0})
1	25.64	111
2	26.92	141
3	25.64	201

In order to reduce the size of the circuit, lumped component pi-network is used to represent each transmission line. The circuit topology is shown in Fig. 5. The circuit composed of one series component and two identical shunt components. The series and shunt components can be inductor or capacitor. If the series component is an inductor and the shunt components are capacitor, the network represents right-handed transmission line. On the other hand, if the series component is a capacitor and the shunt components are inductors, the network represents left-handed transmission line. The lumped components of the circuit are shown in Table 3.2.

Table 3.2 Lumped Components of the Transmission Lines

Transmission Line	Series Component	Shunt Components
1	Capacitor: 3.89 pF	Inductor: 0.648 nH
2	Inductor: 1.13 nH	Capacitor: 6.9 pF
3	Inductor: 1.13 nH	Capacitor: 0.986 pF

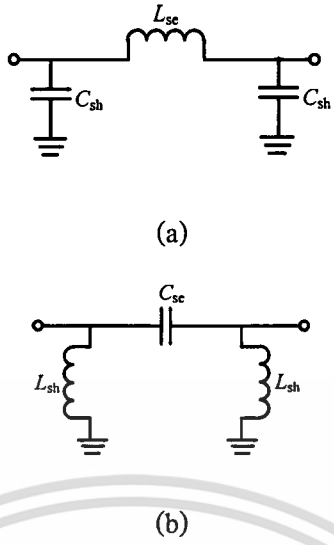

Fig. 3.5 Lumped transmission line topologies consist of (a) right-handed transmission line and (b) left-handed transmission line.

Figure 3.6 shows the schematic of the lumped component rat-race coupler. All the lumped components are then implemented on IPD process. Inductors are implemented by rectangular spiral shape while capacitors are implemented by parallel-plate type. The chip photo is shown in Fig. 3.7.

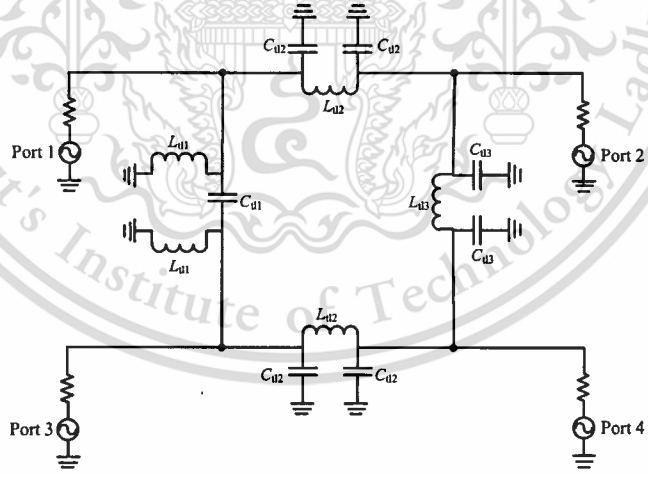

Fig. 3.6 Rat-race circuit with ideal lumped transmission line components.

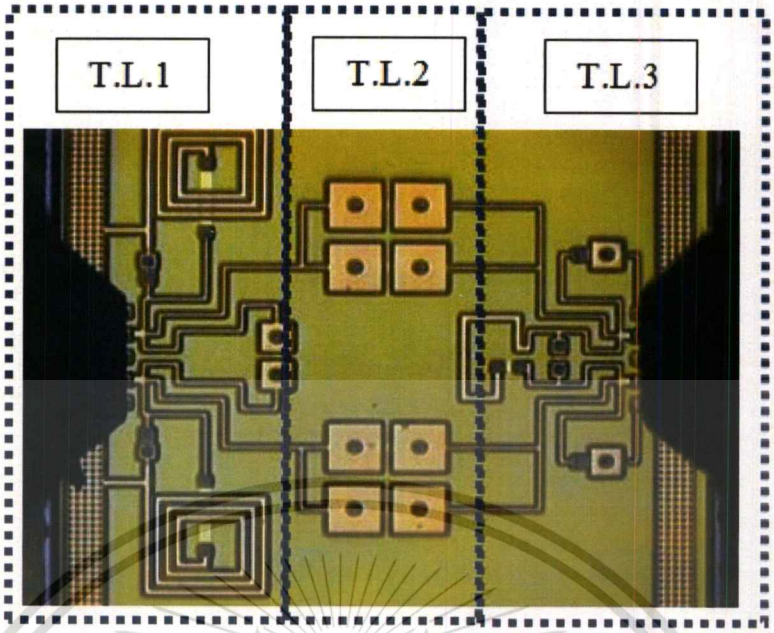

Fig. 3.7 Rat-race circuit photo on IPD process.

To check the performance of the circuit, the simulation results of the ideal lumped component rat-race circuit are compared with the post-simulation results from the circuit implemented on IPD process. The simulation uses frequency range of 1.5-3.5 GHz. The port impedance is fixed at $6.4 + j10\ \Omega$ in the simulated frequency range. The rat-race parameters (eq. 1-4) are shown in Fig. 3.8. The implemented circuit is measured using network analyzer. The measurement results are also compared with the simulation results shown in Fig. 3.8.

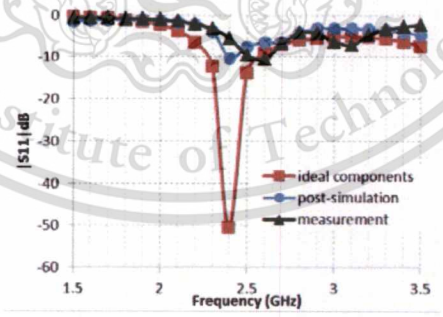

(a)

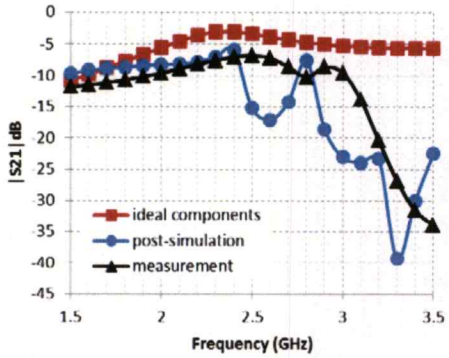

(b)

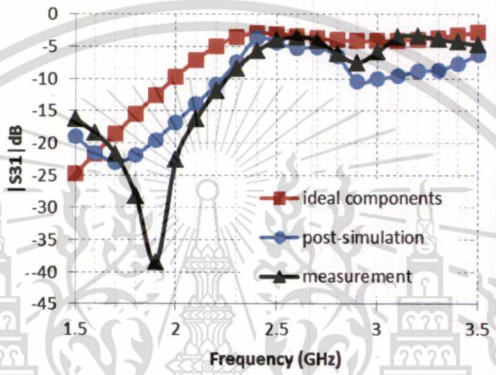

(c)

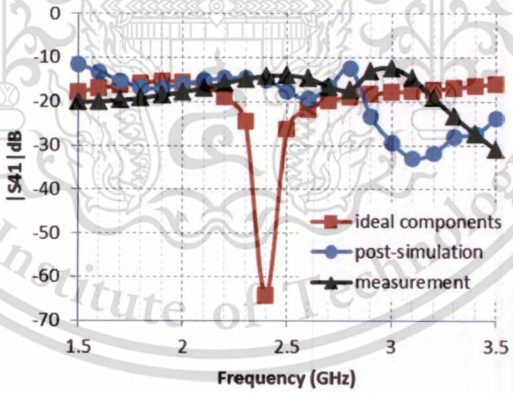

(d)

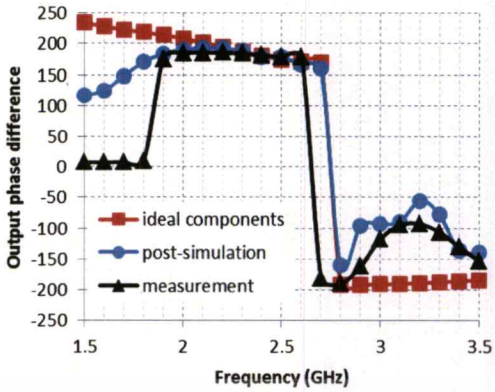

(e)

Fig. 3.8 Rat-race circuit simulation for ideal components and layout on IPD process of (a) $S_{11,dB}$,(b) $S_{21,dB}$(c) $S_{31,dB}$(d) $S_{41,dB}$ (e) phase difference between S_{21} and S_{31}.

From Fig. 3.8, the ideal lumped components yield as low as 50 dB of S_{11} while that of the layout IPD and the measured chip is -10.2 dB and -5.6 dB, respectively. The layout IPD therefore has some reflected power at the input port. The transmission coefficients at port 2 are -3 dB, -5.8 dB and -6.9 dB for the ideal lumped components, the layout IPD simulation and the measured chip, respectively. The transmission coefficients at port 3 are -3 dB, -3.7 dB and -5.7 dB for the ideal lumped components, the layout IPD simulation and the measured chip, respectively. The output powers at the output ports of those three above cases differ by 0.002 dB, 2.1 dB and 1.2 dB, respectively. The transmission coefficients at port 4 are -64 dB, -15 dB and -14 dB for the ideal lumped components, the layout IPD simulation and the measured chip, respectively. Therefore, there is some power provided to the isolation port. Finally, the phase difference at the output ports are 180^{o}, 178.5^{o}, 181.5^{o} for the ideal lumped components, the layout IPD simulation and the measured chip, respectively. Therefore the phase difference values at the output ports are less than 2^{o} in all cases.

The discrepancies between the ideal components and the post-simulation are due to the additional ground loop. While the discrepancies between the post-simulation and the measurement are caused by the parasitic inductance of the whole chip, e.g., mutual coupling between inductance loops in the chip.

3.3. Conclusions

The rat-race coupler with complex termination is implemented on IPD process. The rat-race circuit properties are matching input port, yielding power balance and phase balance at the

output port. The design equations for distributed structure are provided for single frequency operation. To implement the circuit on IPD process, lumped component design is also illustrated. The measured results show -5.6 dB reflection coefficient at the input port, -14 dB transmission coefficient at the isolation port, the transmission coefficient at the output ports is better than -7 dB, and the phase difference at the output ports is less than 2 degrees. The measured results differ from the post-simulation due to parasitic inductance in the chip. Isolation circuit such as guard ring might be included for better performance.

Chapter 4

Conclusions

Rat-race coupler circuits with complex termination are analyzed and designed for single and dual band of frequencies. One is implemented on printed circuit board (PCB) which works on 450/900 MHz. The other is implemented on Integrated Passive Device (IPD) process which works on 2.4 GHz. Both of the circuits use lumped components to minimize the size of the circuits.

For the PCB implementation, a compact 450/900-MHz dual-band rat-race coupler with complex impedance load is designed, implemented, and measured. Lumped components are used to implement transmission line sections in the rat-race design for circuit miniaturization. The circuit simulation shows good performance at both frequencies. The measured circuit also shows good rat-race functions with slightly different performance from the simulation due to two factors: 1) using available lumped components to replace ideal values and 2) lossy lumped components, especially the losses in inductors.

For the IPD process implementation, the rat-race coupler with complex termination is analyzed and designed. The rat-race circuit properties are matching input port, yielding power balance and phase balance at the output port. The design equations for distributed structure are provided for single frequency operation. To implement the circuit on IPD process, lumped component design is also illustrated. The measured results show -5.6 dB reflection coefficient at the input port, -14 dB transmission coefficient at the isolation port, the transmission coefficient at the output ports is better than -7 dB, and the phase difference at the output ports is less than 2 degrees. The measured results differ from the post-simulation due to parasitic inductance in the chip. Isolation circuit such as guard ring might be included for better performance.

Summary of outputs

1) C. Pakasiri, S. Wang, "A compact UHF dual-band rat-race coupler with complex impedance load," Microwave and Optical Technology Letters, vol. 60, pp. 2517-2522, 2018. (ISI: impact factor (2017) 0.948)

2) C. Pakasiri, S. Wang, "2.4 GHz rat-race coupler with complex termination on IPD process," 18th Intl. Symp. On Communicatons and Information Technologies (ISCIT 2018). (will be in Scopus index)

บรรณานุกรม/เอกสารอ้างอิง

Chapter 2

[1] A. Bekasiewicz, S. Koziel, and W. Zieniutycz, "A structure and design optimization of novel compact microscip dual-band rat-race coupler with enhanced bandwidth," Microwave Opt Technol Lett 58 (2016), 2287-2291.

[2] R. Sinha, A. De and S. Sanyal, "A theorem on asymmetric structure based rat-race coupler," IEEE Microw Compon Lett 25 (2015), 145-147.

[3] Q. He, et al., "A novel 180 ° rat-race hybrid with arbitrary power division for complex impedances," Journal of Electromagnetic Waves and Applications (2013), 318-329.

[4] T.-M. Shen, et al., "Design of lumped rat-race coupler in multilayer LTCC," Asia-Pacific Microw. Conf. Digest.(2009), 2120-2123.

[5] S. Wang and J. Y. Zhong, "A compact 2.4/5.2 GHz rat-race coupler on glass substrate," Progress in Electromagnetics Research Letters, vol. 24, pp. 109-118, 2011.

[6] B. Tang, et al., Miniaturized rat-race hybrid incorporating six lumped element components, Microwave Opt Technol Lett 58 (2016), 1125-1128.

[7] C.-H. Tseng, C.-H. Mou, C.-C. Lin and C.-H. Chao, Design of microwave dual-band rat-race couplers in printed-circuit board and GIPD technologies, IEEE Trans Compon. Packag.

Chapter 3

[1] D. M. Pozar, Microwave Engineering, 2nd ed. John Wiley & Sons: U.S.A., 1998, pp.401–411.

[2] R. C. Frye, S. Kapur, and R. C. Melville, "A 2-GHz quadrature hybrid implemented in CMOS technology," IEEE J. Solid-state Circuits, vol. 38, no. 3, pp. 550-555, March 2003.

[3] D. Ozis, J. Paramesh, and D. J. Allstot, "Analysis and design of lumped-element quadrature couplers with lossy passive elements," 2006 IEEE International Symposium on Circuits and Systems, 21-24 May 2006.

[4] T-M. Shen, C.-R. Chen, T.-Y. Huang, and R.-B. Wu, "Design of lumped rat-race coupler in multilayer LTCC," 2009 Asia Pacific Microwave Conference, 7-10 Dec. 2009.

[5] S. Wang, and J.-Y. Zhong, "A compact 2.4/5.2-GHz rat-race coupler on glass substrate," Prog. In Electromagnetics Research Letters, vol. 24, pp.109-118, 2011.

[6] T. Vaha-Heikkila, et al., "Integrated passive device process for high quality factor passive components and modules," 2013 European Microwave Conference, 6-10 Oct. 2013.

[7] Q. He, et al., "A novel 180° rat-race hybrid with arbitrary power division for complex impedance," Journal of Electromagnetic Waves and Applications, pp.318-329, Nov. 2012.

ภาคผนวก ก

สรุปค่าใช้จ่ายการดำเนินโครงการวิจัย

สัญญาเลขที่ KREF156101

โครงการ **วงจรกระจายสัญญาณสำหรับเครือข่ายไร้สาย**

Coupler Circuit for Wireless Application

รายงานสรุปการเงินรอบ 10 เดือน

ชื่อหัวหน้าโครงการวิจัย ผู้รับทุน นาย ฉัตรพล ภคศิริ

รายงานในช่วงตั้งแต่วันที่ 5 ก.พ. 2561 ถึงวันที่ 15 พ.ย. 2561

สรุปงบประมาณค่าใช้จ่ายที่ใช้นับตั้งแต่เริ่มทำการวิจัยถึงปัจจุบัน

หมวดค่าใช้จ่าย	งบประมาณรวม ทั้งโครงการ	ค่าใช้จ่าย จากรายงานครั้งก่อน	ค่าใช้จ่าย งวดปัจจุบัน	รวมค่าใช้จ่าย สะสมถึงปัจจุบัน	คงเหลือ (หรือเกิน)
งบดำเนินงาน					
ค่าใช้สอย	325,500	207,844.71	62,000	269,845	55,655
ค่าวัสดุ	40,000	2534.34	38,866	41,401	(1,401)
รวม	365,500	210,379.05	100,866	311,245	54,254

จำนวนเงินที่ได้รับและจำนวนเงินที่ใช้จ่าย

งวดเงินที่ได้รับ	จำนวนเงินที่ได้รับ(บาท)	เมื่อ (ระบุวัน เดือน ปี)
งวดที่ 1	347,225	6 มี.ค. 2561
งวดที่ 2	-	-
ดอกเบี้ย ครั้งที่ 1		
รวม	347,225	❶

งวดที่	จำนวนเงินที่ใช้จ่าย (บาท)	
งวดที่ 1	210,379.05	
งวดที่ 2	100,866	
รวม	311,245	❷

จำนวนเงินคงเหลือ ❶ - ❷ 35,980 **บาท**

.....	.....
ลงนามหัวหน้าโครงการวิจัยผู้รับทุน โครงการ	**ลงนามเจ้าหน้าที่การเงิน**

ภาคผนวก ข
ผลผลิตที่ได้จากงานวิจัย

Received: 13 February 2018
DOI: 10.1002/mop.31358

A compact UHF dual-band rat-race coupler with complex impedance load

Chatrpol Pakasiri[1] | Sen Wang[2]

[1]College of Advanced Manufacturing Innovation, King Mongkut's Institute of Technology Ladkrabang, Bangkok, Thailand

[2]Department of Electronic Engineering, National Taipei University of Technology, Taipei, Taiwan

Correspondence
Chatrpol Pakasiri, College of Advanced Manufacturing Innovation, King Mongkut's Institute of Technology Ladkrabang, 1 Soi Chalongkrung 1, Ladkrabang, Bangkok, Thailand.
Email: chatrpol.pa@kmitl.ac.th

Funding information
King Mongut's Institute of Technology Ladkrabang and National Taipei University of Technology-King Mongkut's Institute of Technology Ladkrabang Joint Research Program, Grant/Award Numbers: NTUT-KMITL-107-01, KREF156101; Memorandum of Understanding

Abstract

A compact UHF dual-band rat-race coupler with complex terminated loads is proposed. The design procedure starts with design circuit with transmission line (TL) components, and design equations are also detailed in this letter for dual-band operation. Moreover, the circuit size is further reduced by replacing the TLs with lumped components. An example circuit operating at 450/900 MHz is given. The measurement shows that the circuit has the reflection coefficient at the input port less than −13 dB, the transmission coefficient greater than −5.6 dB and phase difference less than ±10° at the output ports.

KEYWORDS
complex load, dual-band, rat-race coupler, UHF

1 | INTRODUCTION

Rat-race coupler circuits are used in many circuit blocks such as low noise amplifier, power splitter, etc. The circuits have been implemented in many forms, for example, on printed-circuit board (PCB), on CMOS platform or on Integrated Passive Device (IPD) platform. On PCB, the circuits have been studied in distributed types[1–3] and lumped component types.[4–6] A combination of distributed and lumped component types are reported in ref.[7] Each platform provides different advantages over various applications. Each platform provides different advantages over various applications. For lumped component types, the circuit size can be made smaller compared with distributed types.

Most of the times, rat-race circuit needs to be integrated with other circuits. Therefore, the terminated loads are usually complex impedance loads. The requirement for rat-race circuits to work with complex impedance loads is of great benefits. In 2013, He et al.[3] proposed novel 180° rat-race hybrid with arbitrary power division for complex impedances. The circuit operates at single frequency with all ports terminated with identical complex loads. The signals at two output ports are equal in magnitude and in phase while that of the other output port is null. In this paper, a compact dual-band rat-race coupler with complex impedance loads is proposed. The example circuits work at 450/900 MHz with output signals being out of phase. The proposed theory of the circuit is based on transmission lines (TLs) and the circuit is transformed to lumped components for further size reduction.

2 | DUAL-BAND RAT-RACE COUPLER WITH COMPLEX IMPEDANCE TERMINAL LOAD

In this section, the dual-band rat-race coupler with complex load is designed and analyzed by using TLs. Properties of the three TLs in the circuit are identified. Then all three TLs are transformed to lumped component circuits. The transformation equations to two types of lumped circuits are given.

2.1 | Dual-band rat-race coupler design with transmission lines

Figure 1 shows the proposed dual-band rat-race coupler, and all four ports are terminated with the same complex load value of Z_L. The load impedance values at the first and second operating frequency are defined as $Z_{L1} = R_{L1} + jX_{L1}$

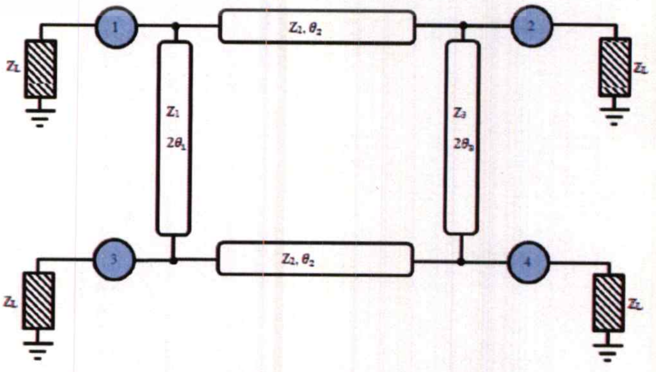

FIGURE 1 The proposed rat-race coupler with complex load termination, Z_L [Color figure can be viewed at wileyonlinelibrary.com]

and $Z_{L2} = R_{L2} + jX_{L2}$, respectively. The first TL has characteristic impedance Z_1 with electrical length $2\theta_1$ at the frequency of interest. Similarly, the second TL has characteristic impedance Z_2 with electrical length θ_2 and the third TL features characteristic impedance Z_3 with electrical length $2\theta_3$. The circuit properties are defined as follows.

$$S_{11} = 0, \tag{1}$$

$$|S_{21}| = |S_{31}|, \tag{2}$$

$$\angle S_{21} - \angle S_{31} = \pm 180^{\circ}, \tag{3}$$

$$S_{41} = 0. \tag{4}$$

By applying even and odd mode analysis, the circuit can be replaced by half-circuits as shown in Figure 2.

The $[ABCD]_e$ matrix of the even mode can be calculated as

$$A_e = \cos(\theta_2) - \frac{Z_2 \sin(\theta_2)\tan(\theta_3)}{Z_3}, \tag{5a}$$

$$B_e = jZ_2 \sin(\theta_2), \tag{5b}$$

$$C_e = j\left[\frac{\cos(\theta_2)\tan(\theta_1)}{Z_1} + \frac{\sin(\theta_2)}{Z_2} - \frac{jZ_2 \sin(\theta_2)\tan(\theta_1)\tan(\theta_3)}{Z_1 Z_3} + \frac{\cos(\theta_2)\tan(\theta_3)}{Z_3}\right], \tag{5c}$$

$$D_e = \frac{-Z_2}{Z_1}\sin(\theta_2)\tan(\theta_1) + \cos(\theta_2). \tag{5d}$$

Similarly, the $[ABCD]_o$ matrix of the odd mode can be calculated as

$$A_o = \cos(\theta_2) - \frac{Z_2 \sin(\theta_2)}{Z_3 \tan(\theta_3)}, \tag{6a}$$

$$B_o = jZ_2 \sin(\theta_2), \tag{6b}$$

$$C_o = j\left[\frac{-\cos(\theta_2)}{Z_1 \tan(\theta_1)} + \frac{\sin(\theta_2)}{Z_2} - \frac{jZ_2 \sin(\theta_2)}{Z_1 Z_3 \tan(\theta_1)\tan(\theta_3)} - \frac{\cos(\theta_2)}{Z_3 \tan(\theta_3)}\right], \tag{6c}$$

$$D_o = \frac{Z_2 \sin(\theta_2)}{Z_1 \tan(\theta_1)} + \cos(\theta_2). \tag{6d}$$

From the $[ABCD]$ matrix, the reflection and transmission coefficients of both even and odd modes can be written as

$$\Gamma_e = \frac{A_e Z_L + B_e - C_e |Z_L|^2 - D_e Z_L^*}{A_e Z_L + B_e + C_e Z_L^2 + D_e Z_L}, \tag{7a}$$

$$\Gamma_o = \frac{A_o Z_L + B_o - C_o |Z_L|^2 - D_o Z_L^*}{A_o Z_L + B_o + C_o Z_L^2 + D_o Z_L}, \tag{7b}$$

$$\tau_e = \frac{2\mathrm{Re}(Z_L)}{A_e Z_L + B_e + C_e Z_L^2 + D_e Z_L}, \tag{7c}$$

$$\tau_o = \frac{2\mathrm{Re}(Z_L)}{A_o Z_L + B_o + C_o Z_L^2 + D_o Z_L}. \tag{7d}$$

Then desired S-parameters of the circuit are

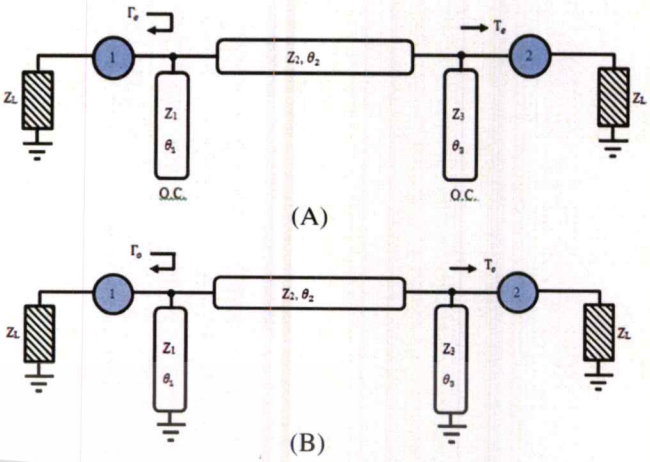

FIGURE 2 Equivalent circuit for (A) even-mode analysis and (B) odd-mode analysis [Color figure can be viewed at wileyonlinelibrary.com]

$$S_{11} = \frac{1}{2}(\Gamma_e + \Gamma_o), \tag{8a}$$

$$S_{21} = \frac{1}{2}(\Gamma_e + \Gamma_o), \tag{8b}$$

$$S_{31} = \frac{1}{2}(\Gamma_e - \Gamma_o), \tag{8c}$$

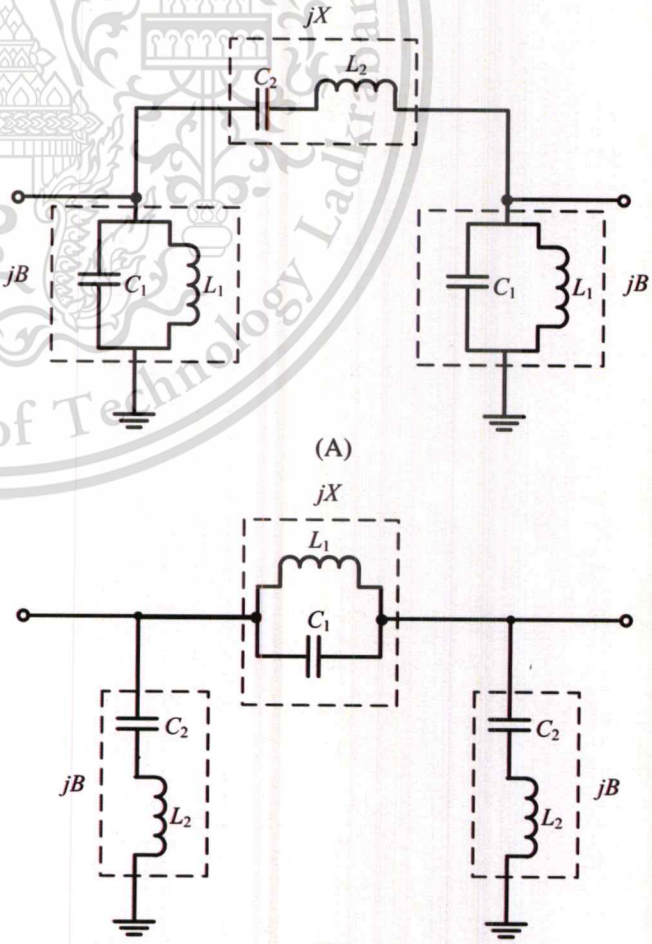

FIGURE 3 (A) Band-pass circuit and (B) band-stop circuit topologies of a T.L

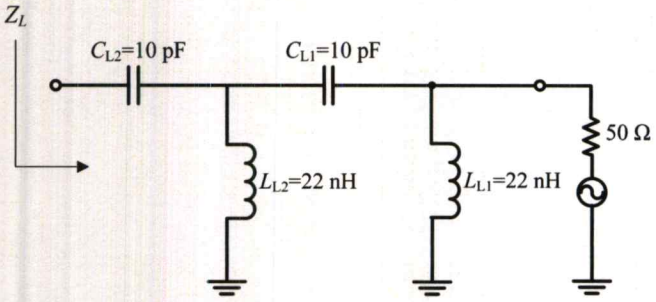

FIGURE 4 Load transformation network

$$S_{41} = \frac{1}{2}(\tau_e - \tau_o). \tag{8d}$$

The relationships between S-parameters in Equation 8 and ABCD-parameters in Equations 5-7 were calculated in ref.[1] It was found in ref.[1] that the relationships between the first and third TL are

$$Z_1 = Z_3 = m, \tag{9}$$

$$\theta_3 = \theta_1 + \frac{\pi}{2} + n\pi. \tag{10}$$

Therefore, the unknown parameters for rat-race circuit are reduced to four unknowns (m, θ_1, Z_2, θ_2) for each operating frequency. To achieve the rat-race circuit conditions in Equations 1-4, four equations must be satisfied as follows:

$$Z_2 \sin(\theta_2) = -m \cdot \sin(2\theta_1), \tag{11}$$

$$\begin{aligned}&\left[\cos(\theta_2) - \frac{Z_2}{m}\sin(\theta_2)\tan\left(\theta_1 + \frac{\pi}{2}\right)\right]X_{L1} + Z_2\sin(\theta_2)\\ &-\left[\frac{\cos(\theta_2)\tan(\theta_1)}{m} + \frac{\sin(\theta_2)}{Z_2}\right.\\ &\qquad\left.-\frac{Z_2}{m^2}\sin(\theta_2)\tan(\theta_1)\tan\left(\theta_1 + \frac{\pi}{2}\right),\right. \qquad (12)\\ &\left.+\frac{\cos(\theta_2)\tan\left(\theta_1 + \frac{\pi}{2}\right)}{m}\right](R_{L1}^2 + X_{L1}^2),\\ &+\left[-\frac{Z_2}{m^2}\sin(\theta_2)\tan(\theta_1) + \cos(\theta_2)\right]X_{L1} = 0\end{aligned}$$

$$Z_2 \sin(k\cdot\theta_2) = -m \cdot \sin(k\cdot 2\theta_1), \tag{13}$$

$$\begin{aligned}&\left[\cos(k\cdot\theta_2) - \frac{Z_2}{m}\sin(k\cdot\theta_2)\tan\left(k\cdot\theta_1 + \frac{\pi}{2}\right)\right]\\ &X_{L1} + Z_2\sin(k\cdot\theta_2) - \left[\frac{\cos(k\cdot\theta_2)\tan(k\cdot\theta_1)}{m}\right.\\ &+\frac{\sin(k\cdot\theta_2)}{Z_2} - \frac{Z_2}{m^2}\sin(k\cdot\theta_2)\tan(k\cdot\theta_1)\tan\left(k\cdot\theta_1 + \frac{\pi}{2}\right) +\\ &\qquad\left.\frac{\cos(k\cdot\theta_2)\tan\left(k\cdot\theta_1 + \frac{\pi}{2}\right)}{m}\right](R_{L1}^2 + X_{L1}^2)\\ &+\left[-\frac{Z_2}{m^2}\sin(k\cdot\theta_2)\tan(k\cdot\theta_1) + \cos(k\cdot\theta_2)\right]X_{L1} = 0,\end{aligned} \tag{14}$$

TABLE 2 Lumped component values of the transmission line sections

Component circuit #	Transmission line section	C_1, pF	L_1, nH	C_2, pF	L_2, nH
Theoretical circuit	1	9.62	7.024	2.95	20.3
	2	6.18	10.55	4.40	13.16
	3	6.18	10.55	1.48	46.38
Post-simulation circuit	1	3.84	10.77	4.15	11.66
	2	6.09	8.768	1.87	14.41
	3	6.15	11.03	0.57	26.19
Implemented circuit	1	3.9	10	3.9	12
	2	5.8	8.7	1.8	15
	3	5.6	11	0.5	28

where k is the ratio of the second to the first operating frequency, $k = f_2/f_1$. For dual-band operation, all TLs except TL_3 calculated from Equations 11-14 can be realized using conventional microstrip lines. Due to the requirement in Equation 10, a conventional microstrip line cannot satisfy the electrical length requirement of both operating frequencies for TL_3. To solve this problem, lumped circuits are used to replace the TLs. The dual-band and distributed-lumped element transformation will be detailed in the next section.

2.2 | Dual-band rat-race coupler design with lumped components

Consider a TL with Z_0 characteristic impedance. The TL has θ_{f1} electrical length at the first operating frequency and θ_{f2} electrical length at the second operating frequency. To replace a microstrip line with lumped components, two types of circuits are used which are band-pass and band-stop

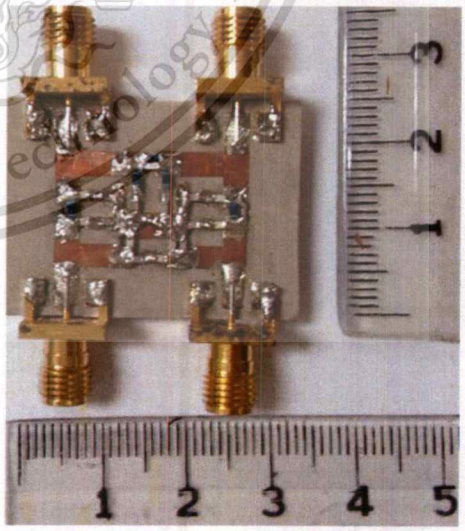

FIGURE 5 Rat-race prototype photo [Color figure can be viewed at wileyonlinelibrary.com]

TABLE 1 Transmission line properties for rat-race coupler with complex load Z_L

Frequency, MHz	Transmission line 1		Transmission line 2		Transmission line 3	
450	$Z_1 = 69.43\ \Omega$	$2\theta_1 = 243^\circ$	$Z_2 = 69.43\ \Omega$	$\theta_2 = 243^\circ$	$Z_3 = 69.43\ \Omega$	$2\theta_3 = 64^\circ$
900	$Z_1 = 69.43\ \Omega$	$2\theta_1 = 127^\circ$	$Z_2 = 69.43\ \Omega$	$\theta_2 = 127^\circ$	$Z_3 = 69.43\ \Omega$	$2\theta_3 = 307^\circ$

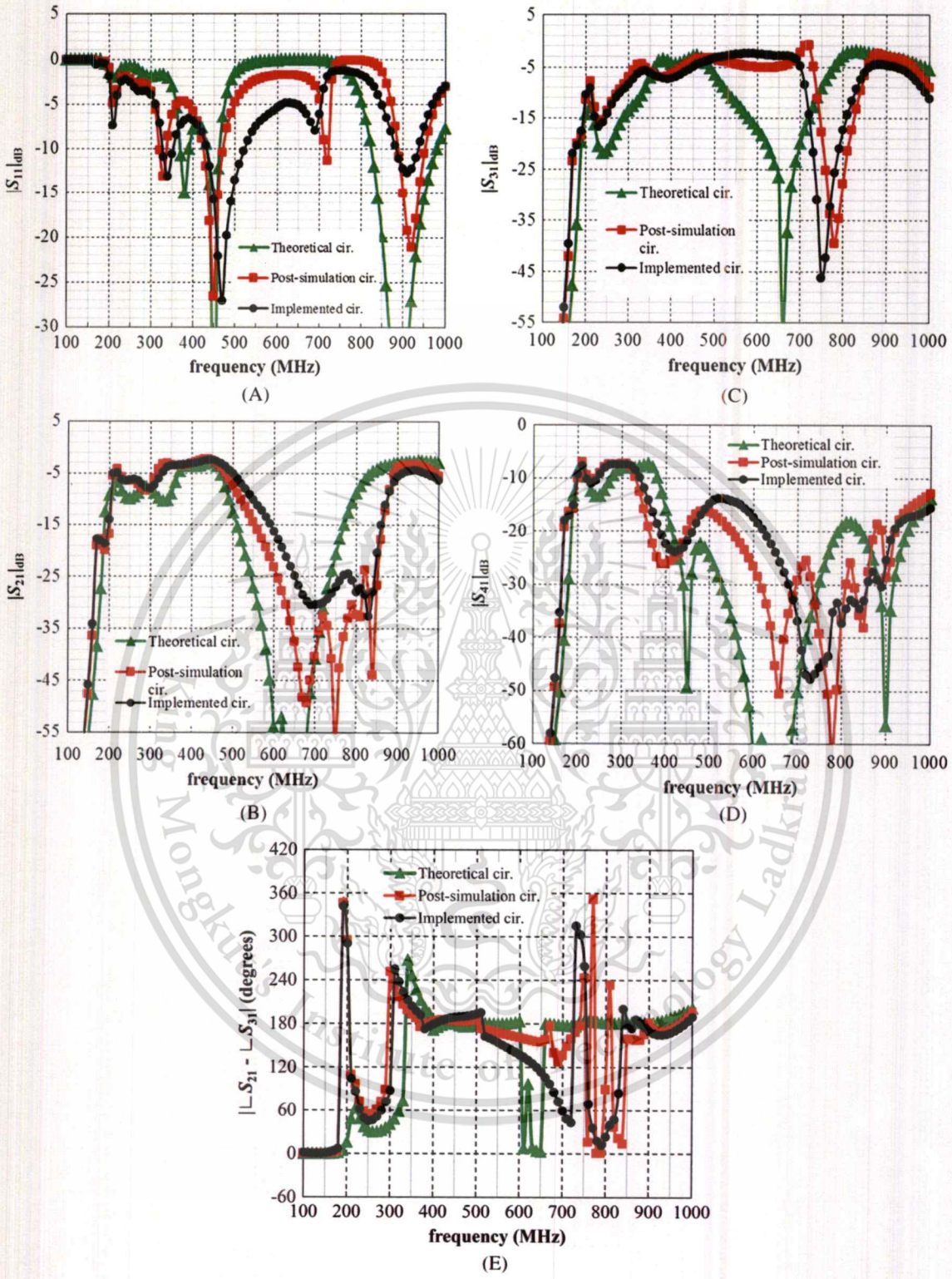

FIGURE 6 *S*-parameters comparison of the rat-race circuits including (a) $|S_{11}|_{dB}$, (B) $|S_{21}|_{dB}$, (C) $|S_{31}|_{dB}$, (D) $|S_{41}|_{dB}$, and (E) $|\angle S_{21}-\angle S_{31}|$ [Color figure can be viewed at wileyonlinelibrary.com]

circuit topologies. Figure 3 shows the lumped circuit TL topologies. For the band-pass topology, the lumped components are related to the TL properties as

$$C_1=\frac{\frac{\omega_1}{Z_o}\left(\csc\left(\theta_{f1}\right)-\cot\left(\theta_{f1}\right)\right)-\frac{\omega_2}{Z_o}\left(\csc\left(\theta_{f2}\right)-\cot\left(\theta_{f2}\right)\right)}{\omega_1^2-\omega_2^2}, \tag{15a}$$

$$L_1=\frac{\frac{1}{\omega_2^2}-\frac{1}{\omega_1^2}}{\frac{1}{Z_o\omega_1}\left(\csc\left(\theta_{f1}\right)-\cot\left(\theta_{f1}\right)\right)-\frac{1}{Z_o\omega_2}\left(\csc\left(\theta_{f2}\right)-\cot\left(\theta_{f2}\right)\right)}, \tag{15b}$$

$$C_2=\frac{\frac{1}{\omega_2^2}-\frac{1}{\omega_1^2}}{\frac{1}{\omega_1}\left(\frac{2}{B_1}-\frac{\sin\left(\theta_{f1}\right)}{Z_oB_1^2}\right)-\frac{1}{\omega_2}\left(\frac{2}{B_2}-\frac{\sin\left(\theta_{f2}\right)}{Z_oB_1^2}\right)}, \tag{15c}$$

TABLE 3 Rat-race circuit performance

Frequency (MHz)	Conditions circuit #	$\lvert S_{11}\rvert_{dB}$	$\lvert S_{21}\rvert_{dB}$	$\lvert S_{31}\rvert_{dB}$	$\lvert S_{41}\rvert_{dB}$	$\lvert\angle S_{21}-\angle S_{31}\rvert$
450	Theoretical	−49	−3	−3	−49	180°
	Post-simulation	−26	−2.6	−3.8	−20	183°
	Implemented	−16	−2.4	−4.9	−22	188°
900	Theoretical	−54	−3	−3	−56	180°
	Post-simulation	−15	−3.8	−3	−15	181°
	Implemented	−13	−5.6	−4.5	−25	170°

$$L_2=\frac{\omega_1\left(\frac{2}{B_1}-\frac{\sin(\theta_{f1})}{Z_oB_1^2}\right)-\omega_2\left(\frac{2}{B_2}-\frac{\sin(\theta_{f2})}{Z_oB_2^2}\right)}{\omega_1^2-\omega_2^2}, \tag{15d}$$

where ω_1 and ω_2 are angular frequencies at the first and second operating frequencies, respectively. The susceptance (B_1) at the first frequency and the susceptance (B_2) at the second frequency are related to the TL properties as

$$B_1=\frac{1}{Z_o}\left(\csc(\theta_{f1})-\cot(\theta_{f1})\right), \tag{16a}$$

$$B_2=\frac{1}{Z_o}\left(\csc(\theta_{f2})-\cot(\theta_{f2})\right). \tag{16b}$$

For the band-stop topology, the lumped components are related to the TL properties as

$$C_1=\frac{1}{\omega_2^2-\omega_1^2}\left[\frac{\omega_1}{\left(\frac{2}{B_1}-\frac{\sin(\theta_{f1})}{Z_oB_1^2}\right)}-\frac{\omega_2}{\left(\frac{2}{B_2}-\frac{\sin(\theta_{f2})}{Z_oB_2^2}\right)}\right], \tag{17a}$$

$$L_1=\frac{\frac{1}{\omega_1^2}-\frac{1}{\omega_2^2}}{\frac{1/\omega_1}{\left(\frac{2}{B_1}-\frac{\sin(\theta_{f1})}{Z_oB_1^2}\right)}-\frac{1/\omega_2}{\left(\frac{2}{B_2}-\frac{\sin(\theta_{f2})}{Z_oB_2^2}\right)}}, \tag{17b}$$

$$C_2=\frac{\frac{1}{\omega_1^2}-\frac{1}{\omega_2^2}}{\frac{Z_o/\omega_1}{\csc(\theta_{f1})-\cot(\theta_{f1})}-\frac{Z_o/\omega_2}{\csc(\theta_{f2})-\cot(\theta_{f2})}}, \tag{17c}$$

$$L_2=\frac{\frac{\omega_1Z_o}{\csc(\theta_{f1})-\cot(\theta_{f1})}-\frac{\omega_2Z_o}{\csc(\theta_{f2})-\cot(\theta_{f2})}}{\omega_2^2-\omega_1^2}. \tag{17d}$$

In the next section, all three TLs in the rat-race circuit are designed with lumped components. The dual-band rat-race coupler operates at 450 MHz and 900 MHz.

3 | IMPLEMENTATION AND MEASUREMENTS

An example circuit is designed with a complex impedance load. The rat-race circuit is designed to operate at 450 MHz (f_1) and 900 MHz (f_2). To implement a complex terminal at the rat-race port, a transformation circuit consisting of L-C ladder network shown in Figure 4 is used. The source impedance is assumed to be 50 Ω. The load values at both operating frequencies are calculated to be $Z_L(f_1) = 33.11 - j29.04\ \Omega$ and $Z_L(f_2) = 38.65 - j4.65\ \Omega$.

Using the design Equations (9)-(14), the properties of all three TLs are tabulated in Table 1. Then applying Equations 15-17, ideal lumped components values are also shown in Table 2 as theoretical circuit. The circuits are implemented on a PCB from Rogers Corporation, RO3010 having relative dielectric constant (ε_r) of 10.2 and loss tangent of 0.0022. The board thickness is 1.27 mm. To incorporate the PCB traces in the circuit, the layout of the circuit are simulated by Momentum in Advanced Design System (ADS). Then all lumped components are adjusted accordingly. The results are also shown in Table 2 as post-simulation circuit. In addition, the implemented circuit shown in the table uses practical lumped components for experiment. The prototype unit is shown in Figure 5. The circuit size is 2.5×3.4 cm^2, which is $0.075\lambda_2\times0.102\lambda_2$ where λ_2 is wavelength at 900 MHz.

Using complex ports shown in Figure 4, the *S*-parameters of the rat-race circuits are shown in Figure 6. Table 3 summarizes the circuit performance at 450 MHz and 900 MHz. From the table, the theoretical circuit shows excellent performance as it meets all conditions in Equations 1-4. With the layout integrated into the circuit, the performance of the post-simulation circuit is dropped. For the prototype unit, the performance of implemented circuit is dropped further. The lower performance of the post-simulation from the implemented circuit is caused by both using practical lumped components and having parasitic loss in components, especially the inductors.

4 | CONCLUSION

In this letter, a compact 450/900-MHz dual-band rat-race coupler with complex impedance load is designed, implemented, and measured. Lumped components are used to implement TL sections in the rat-race design for circuit miniaturization. The circuit simulation shows good performance at both frequencies. The measured circuit also shows good rat-race functions with slightly different performance from the simulation due to two factors: (1) using available lumped components to replace ideal values and (2) lossy lumped components, especially the losses in inductors. The proposed methodology is promising in design dual-band rat-race coupler with complex load termination.

ACKNOWLEDGMENTS

This project is supported by the Research Funding under the Memorandum of Understanding, KREF156101, of King Mongut's Institute of Technology Ladkrabang and National Taipei University of Technology-King Mongkut's Institute

of Technology Ladkrabang Joint Research Program under Grant NTUT-KMITL-107-01.

ORCID

Chatrpol Pakasiri http://orcid.org/0000-0002-0387-8105

REFERENCES

[1] Bekasiewicz A, Koziel S, Zieniutycz W. A structure and design optimization of novel compact microscip dual-band rat-race coupler with enhanced bandwidth. *Microwave Opt Technol Lett.* 2016; 58:2287-2291.

[2] Sinha R, De A, Sanyal S. A theorem on asymmetric structure based rat-race coupler. *IEEE Microw Compon Lett.* 2015;25:145-147.

[3] He Q, Liu YA, Li SL, Su M, Wu YL. A novel 180° rat-race hybrid with arbitrary power division for complex impedances, journal of electromagnetic waves and applications 2013;25:318-329.

[4] Shen T-M, Chen CR, Huang TY, Wu RB. Design of lumped rat-race coupler in multilayer LTCC. *Asia-Pacific Microw Conf Digest.* Singapore 2009;2120-2123.

[5] Wang S, Zhong JY. A compact 2.4/5.2 GHz rat-race coupler on glass substrate. *Prog Electromagn Res Lett.* 2011;24:109–118.

[6] Tang B, Hayashi H, Ueda R. Miniaturized rat-race hybrid incorporating six lumped element components. *Microwave Opt Technol Lett.* 2016;58:1125-1128.

[7] Tseng C-H, Mou C-H, Lin C-C, Chao C-H. Design of microwave dual-band rat-race couplers in printed-circuit board and GIPD technologies. *IEEE Trans Compon Packag Manuf Technol.* 2016;6: 262-271.

How to cite this article: Pakasiri C, Wang S. A compact UHF dual-band rat-race coupler with complex impedance load. *Microw Opt Technol Lett.* 2018; 60:2517–2522. https://doi.org/10.1002/mop.31358

Received: 19 February 2018

DOI: 10.1002/mop.31355

Electromagnet-driven long-period fiber gratings for tunable Tm/Ho-codoped silica fiber lasers

Shimpei Dodo | **Keisuke Hashimoto** | **Hajime Sakata**

Department of Electrical and Electronic Engineering, Graduate School of Science and Technology, Shizuoka University, Hamamatsu, Japan

Correspondence
H. Sakata, Department of Electrical and Electronic Engineering, Graduate School of Science and Technology, Shizuoka University, Hamamatsu, Japan.
Email: sakata.hajime@shizuoka.ac.jp

Abstract

We report the experimental results on controlling the oscillation wavelength by inducing force-induced fiber gratings in Tm/Ho co-doped fiber ring resonators. The fiber grating generates the resonance loss bands that are controlled with an electromagnet. The oscillation wavelength covers from 1879 nm to 1995 nm overall by shifting the passband that appears between the neighboring loss bands.

KEYWORDS

Tm/Ho co-doped silica fibers, tunable fiber lasers

1 | INTRODUCTION

2 μm-band eye-safe lasers attract great interest in the application fields of lidars, gas detection, and medical treatment[1–4]. In these applications, laser wavelength tuning is crucial to expand the usage range. For example, we can access plural absorption peaks of the greenhouse gases, such as carbon dioxide, nitrogen oxide, and water vapor, by tuning the oscillation wavelength. As for the medical purpose, one of absorption peaks of water is located at ~1.94 μm and its absorption coefficient increases toward this peak. The optical penetration depth in tissues is thus controllable by the laser wavelength rather than the output power. The rare-earth ions of Tm^{3+} and Ho^{3+} are most common as the active media used for the 2 μm-band fiber lasers, which covers the wavelength range from 1.75 μm to 2.15 μm[5,6]. The Tm/Ho co-doped fiber lasers (THFLs) is capable of the broad oscillation wavelength range by directly emitting the energy from the $^3F_4$ level to the $^3H_6$ of Tm^{3+} or by transferring the energy from the $^3F_4$ level of Tm^{3+} to the $^5I_7$ level of Ho^{3+}. So far, the wavelength tuning in the 2 μm-band fiber lasers has been realized by using extra-fiber optical instruments, such as rotatable diffraction gratings.[7,8] However, such tunable systems remain the problems like insertion loss, robustness, environmental fluctuation, because of the input and output coupling of light with the fibers. In-fiber tuning mechanism is capable of solving such problems. Thus far, all-fiber tunable lasers in the 2 μm band have been demonstrated using temperature-dependent fused-fiber couplers and using polarization controllers.[9,10] In our previous articles, we have reported the wavelength control with all fiber configurations by incorporating a force-induced long-period fiber grating (LPFG) into the fiber ring resonators including the Er- or Tm-doped fibers.[11,12] In this article, we introduce the force-

2.4 GHz Rat-Race Coupler with Complex Termination on IPD Process

Chatrpol Pakasiri
College of Advanced Manufacturing Innovation
King's Mongkut's Institute of Technology Ladkrabang
Bangkok, Thailand
chatrpol.pa@kmitl.ac.th

Sen Wang
Department of Electronic Engineering
National Taipei University of Technology
Taipei, Taiwan
wangsen@mail.ntut.edu.tw

***Abstract*—This paper proposed a rat-race circuit implement on IPD (Integrated Passive Device) process. The termination loads of the circuit have a complex impedance value. Design equations for single frequency operation of distributed structure are provided. Lumped components representation of distributed structure is illustrated in the design example. The measured results yield -5.6 dB reflection coefficient at the input port and -14 dB transmission coefficient at the isolation port. The transmission coefficients at the output ports are better than -7 dB while the phase difference is less than 2 degrees.**

Keywords—rat-race coupler, complex termination, integrated passive device, IPD.

I. INTRODUCTION

Rat-race coupler are commonly used in microwave circuit. On printed-circuit board, the longest transmission line can be as long as $3\lambda/4$ for normal real termination load [1]. Many researches have been done to minimize the size of the circuit [2-5]. In CMOS process, the quality factor of inductors is usually small, and therefore the performance of circuits is degraded [2]. In LTTC process, performance of circuit is quite good because of availability of high quality factor of inductors. Nevertheless, the production cost of LTTC is relatively high. Integrated passive device (IPD) process becomes more popular because of its relatively low production cost. It also provides high quality factor for passive components and modules [6].

Complex termination is usually encountered in circuit design. In [7], a hybrid rat-race coupler with in phase output ports has been derived for complex termination. In this paper, a proposed rat-race coupler at ISM band is implemented on IPD process. The output port design is modified to have out-of-phase signals. The circuit ports are terminated with a complex impedance value. The input port is matched. There are one isolation port and two output ports with differential signal.

This paper is organized as follows. Section II gives an analysis on complex termination rat-race coupler. Section III shows the implementation on IPD process and simulation results. Section IV draws some conclusions.

II. COMPLEX TERMINATION RAT-RACE COUPLER

A. Rat-Race Coupler Circuit Properties

In this paper, the rat-race circuit properties are defined as follows,

$$S_{11} = 0, \tag{1}$$

$$|S_{21}| = |S_{31}|, \tag{2}$$

$$\angle S_{21} - \angle S_{31} = \pm 180°, \tag{3}$$

$$S_{41} = 0 \tag{4}$$

where the input port is port 1, the output ports are port 2 and port 3 and the isolation port is port 4. Figure 1 shows the proposed rat-race structure. Each port is terminated with a complex impedance value, Z_L.

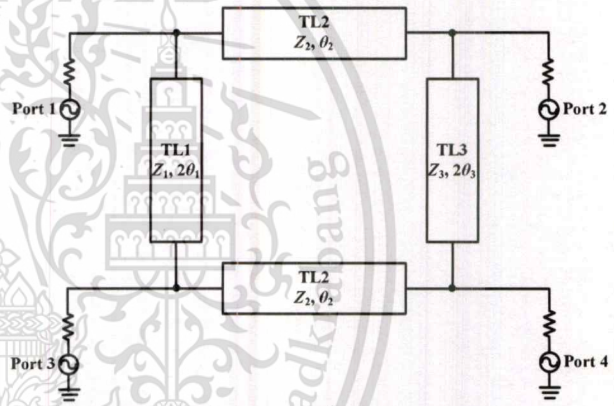

Fig. 1 The proposed rat-race coupler.

Because of the symmetric structure of the circuit, even and odd mode analysis can be applied. The analysis will be described next.

B. Even and Odd mode Analysis

Figure 2 shows the structure when even mode is excited into the circuit. The first and the third transmission lines are separated in half, so does their electrical length. The reflection coefficient for the even mode can be found as

$$\Gamma_e = \frac{Z_{in}^{1e} - Z_L^*}{Z_{in}^{1e} + Z_L}, \tag{5a}$$

where

$$Z_{in}^{1e} = \frac{Z_{x2}^e(-jZ_1\cot(\theta_1))}{Z_{x2}^e + (-jZ_1\cot(\theta_1))}, \tag{5b}$$

$$Z_{x2}^e = Z_2\frac{Z_{x1}^e + jZ_2\tan(\theta_2)}{Z_2 + jZ_{x1}^e\tan(\theta_2)}, \tag{5c}$$

$$Z_{x1}^e = \frac{(-jZ_3\cot(\theta_3))Z_L}{(-jZ_3\cot(\theta_3)) + Z_L}. \tag{5d}$$

Note that * implies complex conjugate operator.

978-1-5386-8458-0/18/$31.00 ©2018 IEEE

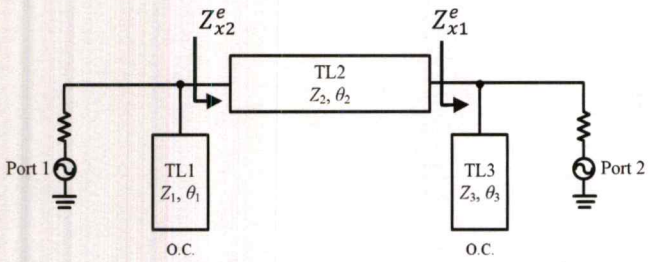

Fig. 2 Rat-race coupler for even mode analysis.

The transmission coefficient

$$T_e = \left(\frac{1+\Gamma_L^e}{e^{j\theta_2}+\Gamma_L^e e^{-j\theta_2}}\right)\left(\frac{Z_{in}^{1e}}{Z_{in}^{1e}+Z_s}\right)\left(1+\frac{Z_L^*}{Z_L}\right), \quad (6a)$$

where

$$\Gamma_L^e = \frac{Z_{x1}^e - Z_2}{Z_{x1}^e + Z_2}. \quad (6b)$$

For the odd mode analysis, Fig. 3 shows the equivalent circuit. The reflection coefficient of the odd mode can be found as

$$\Gamma_o = \frac{Z_{in}^{1o} - Z_L^*}{Z_{in}^{1o} + Z_L}, \quad (7a)$$

where

$$Z_{in}^{1o} = \frac{Z_{x2}^o (jZ_1 \tan(\theta_1))}{Z_{x2}^o + (jZ_1 \tan(\theta_1))}, \quad (7b)$$

$$Z_{x2}^o = Z_2 \frac{Z_{x1}^o + jZ_2 \tan(\theta_2)}{Z_2 + jZ_{x1}^o \tan(\theta_2)}, \quad (7c)$$

$$Z_{x1}^o = \frac{(jZ_3 \tan(\theta_3))Z_L}{(jZ_3 \tan(\theta_3)) + Z_L}. \quad (7d)$$

The transmission coefficient for the odd mode is

$$T_o = \left(\frac{1+\Gamma_L^o}{e^{j\theta_2}+\Gamma_L^o e^{-j\theta_2}}\right)\left(\frac{Z_{in}^{1o}}{Z_{in}^{1o}+Z_s}\right)\left(1+\frac{Z_L^*}{Z_L}\right), \quad (8a)$$

where

$$\Gamma_L^o = \frac{Z_{x1}^o - Z_2}{Z_{x1}^o + Z_2}. \quad (8b)$$

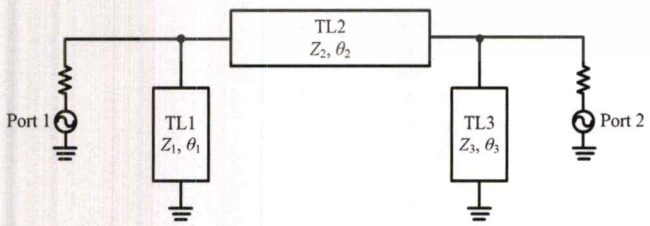

Fig. 3 Rat-race coupler for odd mode analysis.

Then S-parameters of the circuit can be found as

$$S_{11} = 0.5(\Gamma_e + \Gamma_o), \quad (9a)$$

$$S_{21} = 0.5(T_e + T_o), \quad (9b)$$

$$S_{31} = 0.5(\Gamma_e - \Gamma_o), \quad (9c)$$

$$S_{41} = 0.5(T_e - T_o). \quad (9d)$$

The relationships between the first and the third transmission line can be found as

$$Z_3 = Z_1, \quad (10)$$

$$\theta_3 = \theta_1 + \frac{\pi}{2} + n\pi. \quad (11)$$

The relationships between the first and the second transmission line can be found as

$$Z_2 \sin(\theta_2) = -Z_1 \sin(2\theta_1), \quad (12)$$

$$[\cos(\theta_2) - (Z_2/Z_1)\sin(\theta_2)\tan(\theta_1 + \pi/2)]X_{L1} + Z_2 \sin(\theta_2) - \left[\frac{\cos(\theta_2)\tan(\theta_2)}{Z_1} + \frac{\sin(\theta_2)}{Z_2} - \frac{Z_2}{Z_1^2}\sin(\theta_2)\tan(\theta_1)\tan\left(\theta_1 + \frac{\pi}{2}\right) + \frac{\cos(\theta_2)\tan\left(\theta_1 + \frac{\pi}{2}\right)}{Z_1}\right]|Z_L|^2 + \left[-\frac{Z_2}{Z_1^2}\sin(\theta_2)\tan(\theta_1) + \cos(\theta_2)\right]X_{L1} = 0,$$

where

$$Z_L = R_L + jX_L. \quad (14)$$

In the next section, a designed rat-race coupler on IPD process is discussed. The circuit layout is simulated by using ADS.

III. Rat-Race Coupler on IPD Process

The IPD process has three metal layers and two different types of dielectrics. The dielectric 1 and 2 have relative dielectric constant values of 6.7 and 2.65, respectively. The metal and via between the dielectric layers are made of copper. Figure 4 shows the cross section view of the IPD process.

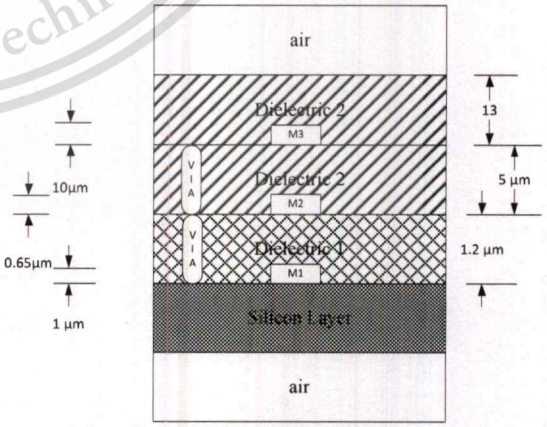

Fig. 4 Cross-section view of the IPD process.

An example circuit is set to have a complex terminal load value of $Z_L = 6.4 + j10\ \Omega$. Using design equations (10)-(13), all the transmission line properties are found and shown in Table I.

TABLE I. TRANSMISSION LINE PROPERTIES OF RAT-RACE CIRCUIT

Transmission Line	Characteristic Impedance (Ω)	Electrical Length (°)
1	25.64	111
2	26.92	141
3	25.64	201

In order to reduce the size of the circuit, lumped component pi-network is used to represent each transmission line. The circuit topology is shown in Fig. 5. The circuit composed of one series component and two identical shunt components. The series and shunt components can be inductor or capacitor. If the series component is an inductor and the shunt components are capacitor, the network represents right-handed transmission line. On the other hand, if the series component is a capacitor and the shunt components are inductors, the network represents left-handed transmission line. The lumped components of the rat-race circuit are shown in Table II.

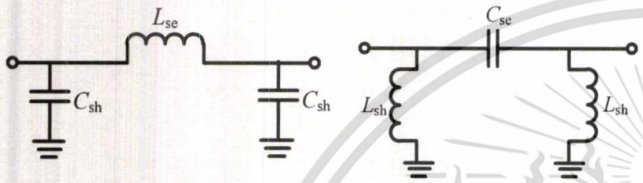

(a) (b)

Fig. 5 Lumped transmission line topologies consist of (a) right-handed transmission line and (b) left-handed transmission line.

TABLE II. LUMPED COMPONENTS OF THE TRANSMISSION LINES

Transmission Line	Series Component	Shunt Components
1	Capacitor: 3.89 pF	Inductor: 0.648 nH
2	Inductor: 1.13 nH	Capacitor: 6.9 pF
3	Inductor: 1.13 nH	Capacitor: 0.986 pF

Figure 6 shows the schematic of the lumped component rat-race coupler. All the lumped components are then implemented on IPD process. Inductors are implemented by rectangular spiral shape while capacitors are implemented by parallel-plate type. The chip photo is shown in Fig. 7.

To check the performance of the circuit, the simulation results of the ideal lumped component rat-race circuit are compared with the post-simulation results from the circuit implemented on IPD process. The simulation uses frequency range of 1.5-3.5 GHz. The port impedance is fixed at $6.4 + j10\ \Omega$ in the simulated frequency range. The rat-race parameters (eq. 1-4) are shown in Fig. 8. The implemented circuit is measured using network analyzer. The measurement results are also compared with the simulation results shown in Fig. 8.

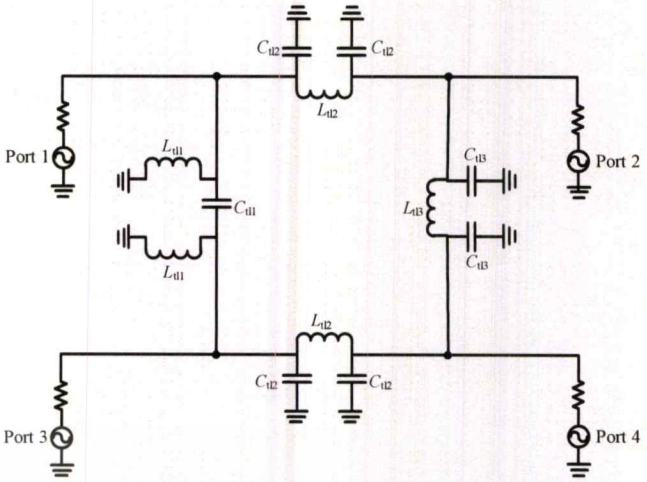

Fig. 6 Rat-race circuit with ideal lumped transmission line components.

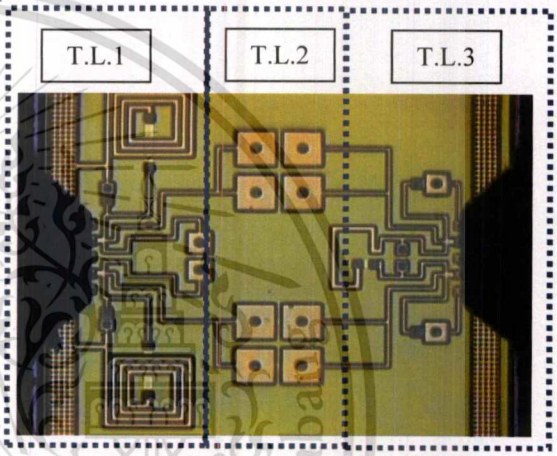

Fig. 7 Rat-race circuit photo on IPD process.

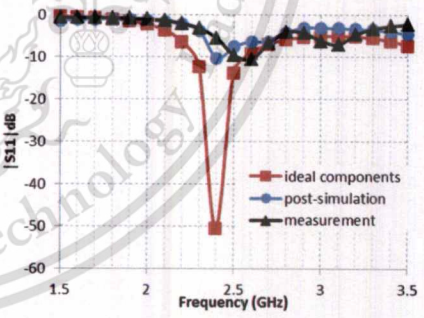

(a)

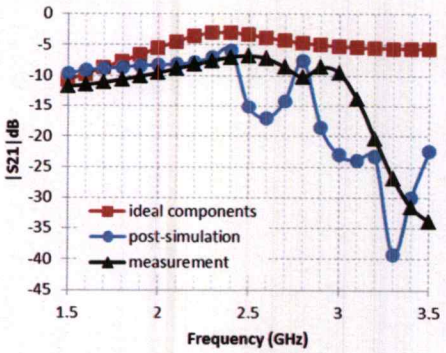

(b)

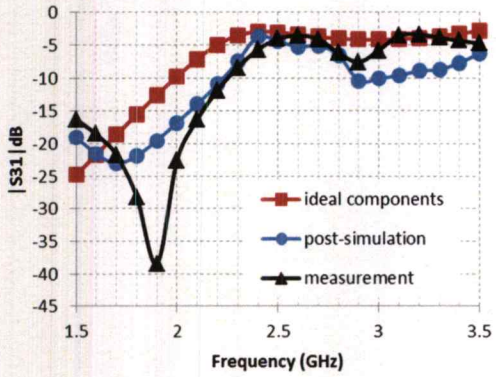

(c)

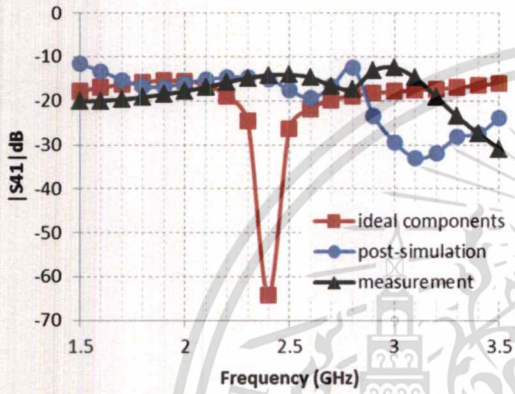

(d)

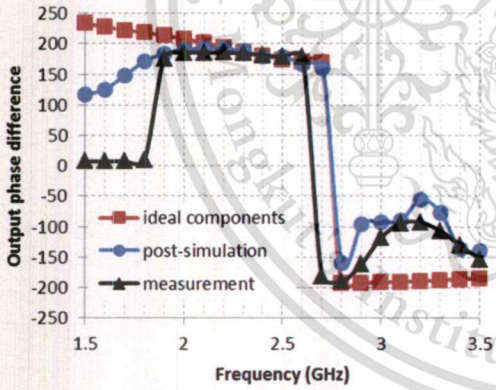

(e)

Fig. 8 Rat-race circuit simulation for ideal components and layout on IPD process of (a) $S_{11,dB}$,(b) $S_{21,dB}$(c) $S_{31,dB}$(d) $S_{41,dB}$ (e) phase difference between S_{21} and S_{31}.

From Fig. 8, the ideal lumped components yield as low as 50 dB of S_{11} while that of the layout IPD and the measured chip is -10.2 dB and -5.6 dB, respectively. The layout IPD therefore has some reflected power at the input port. The transmission coefficients at port 2 are -3 dB, -5.8 dB and -6.9 dB for the ideal lumped components, the layout IPD simulation and the measured chip, respectively. The transmission coefficients at port 3 are -3 dB, -3.7 dB and -5.7 dB for the ideal lumped components, the layout IPD simulation and the measured chip, respectively. The output powers at the output ports of those three above cases differ by 0.002 dB, 2.1 dB and 1.2 dB, respectively. The transmission coefficients at port 4 are -64 dB, -15 dB and -14 dB for the ideal lumped components, the layout IPD simulation and the measured chip, respectively. Therefore, there is some power provided to the isolation port. Finally, the phase difference at the output ports are 180°, 178.5°, 181.5° for the ideal lumped components, the layout IPD simulation and the measured chip, respectively. Therefore the phase difference values at the output ports are less than 2° in all cases.

The discrepancies between the ideal components and the post-simulation are due to the additional ground loop. While the discrepancies between the post-simulation and the measurement are caused by the parasitic inductance of the whole chip, e.g., mutual coupling between inductance loops in the chip.

IV. Conclusions

The rat-race coupler with complex termination is implemented on IPD process. The rat-race circuit properties are matching input port, yielding power balance and phase balance at the output port. The design equations for distributed structure are provided for single frequency operation. To implement the circuit on IPD process, lumped component design is also illustrated. The measured results show -5.6 dB reflection coefficient at the input port, -14 dB transmission coefficient at the isolation port, the transmission coefficient at the output ports is better than -7 dB, and the phase difference at the output ports is less than 2 degrees. The measured results differ from the post-simulation due to parasitic inductance in the chip. Isolation circuit such as guard ring might be included for better performance.

Acknowledgment

This project is supported by the Research Funding under the Memorandum of Understanding, KREF156101, of King Mongut's Institute of Technology Ladkrabang and National Taipei University of Technology-King Mongkut's Institute of Technology Ladkrabang Joint Research Program under Grant NTUT-KMITL-107-01.

References

[1] D. M. Pozar, Microwave Engineering, 2nd ed. John Wiley & Sons: U.S.A., 1998, pp.401–411.

[2] R. C. Frye, S. Kapur, and R. C. Melville, "A 2-GHz quadrature hybrid implemented in CMOS technology," *IEEE J. Solid-state Circuits*, vol. 38, no. 3, pp. 550-555, March 2003.

[3] D. Ozis, J. Paramesh, and D. J. Allstot, "Analysis and design of lumped-element quadrature couplers with lossy passive elements," 2006 *IEEE International Symposium on Circuits and Systems*, 21-24 May 2006.

[4] T-M. Shen, C.-R. Chen, T.-Y. Huang, and R.-B. Wu, "Design of lumped rat-race coupler in multilayer LTCC," *2009 Asia Pacific Microwave Conference*, 7-10 Dec. 2009.

[5] S. Wang, and J.-Y. Zhong, "A compact 2.4/5.2-GHz rat-race coupler on glass substrate," *Prog. In Electromagnetics Research Letters*, vol. 24, pp.109-118, 2011.

[6] T. Vaha-Heikkila, et al., "Integrated passive device process for high quality factor passive components and modules," *2013 European Microwave Conference*, 6-10 Oct. 2013.

[7] Q. He, et al., "A novel 180° rat-race hybrid with arbitrary power division for complex impedance," *Journal of Electromagnetic Waves and Applications*, pp.318-329, Nov. 2012.

ประวัตินักวิจัย

1. ฉัตรพล ภคศิริ

Name-Last Name Chatrpol Pakasiri

Present Position Teacher

Position Title Lecturer

Education

Degree Level	Major	Institute or University	Graduation Year
Ph.D.	Electrical and Computer Engineering	University of Houston, Texas, U.S.A.	2005
M.S.	Electrical Engineering and Computer Science	National Chiao Tung University, Taiwan	2013
M.S.	Electrical and Computer Engineering	University of Houston, Texas, U.S.A.	2001
B.S.	Electronic Engineering	King Mongkut's Institute of Technology Ladkrabang	1996

Point of Contact College of Advanced Manufacturing Innovation, King Mongkut's Institute of Technology Ladkrabang , 1 Soi Chalongkrung 1, Ladkrabang, Bangkok, Thailand 10520

Research Experience or Field of Expertise Microwave passive and active circuit, antenna design, numerical electromagnetics

Work/Experience

Research Output/Creative Work/Innovations/Patents

- Projects & Patents:
  - Directive magnetic antenna for HF band (3 MHz – 30 MHz) (Thai Petty Patent Submitting)
  - Study of DC motor simulation
  - Design of power amplifier at 900 MHz
- Selected Publication lists (International Journals)

[1] Chao-Han Tsai ,I-No Liao , Pakasiri, C., Hsin-Cheng Pan , Yu-Jiu Wang, "A Wideband 20 mW UHF Rectifier in CMOS," IEEE Microwave and Wireless Components Letters, vol. 25, pp. 388-390, June 2015.

[2] Wang, Y.J., Liao, I-No, Tsai, C.H., Pakasiri, C., "A Millimeter-Wave In-Phase Gate-Boosting Rectifier," IEEE Trans. Micro. Theo. Tech., pp. 2768-2783, Nov 2014.

[3] Pakasiri, C. and Torrungrueng, D., "Forward-backward Method with a Spectral Acceleration Algorithm for Capacitance Extraction of Planar Structures on a Single-Layered Medium," Microwave and Optical Technology Letters, vol. 56, no. 3, March 2014, pp. 694-700.

[4] Lertsirimit, C. and Torrungrueng, D., "Fast capacitance extraction for finite planar periodic structures using the generalized forward-backward and novel spectral acceleration method," Progress In Electromagnetics Research, vol. 96, pp. 251-266,2009.

2. Sen Wang

Name-Last Name Sen Wang

Present Position Teacher

Position Title Professor

Education

Degree Level	Major	Institute or University	Graduation Year
Ph.D.	Communication Engineering	National Taiwan University	2009
M.S.	Communication Engineering	National Taiwan University	2006
B.S.	Electrical Engineering	National Taiwan University	2004

Point of Contact Microwave/Millimeter-wave Integrated Circuits Lab., Department of Electronic Engineering, National Taipei University of Technology, 1, Sec. 3, Zhongxiao E. Rd., Taipei, 10608, Taiwan

Research Experience or Field of Expertise Integrated circuit designs for research and development of RF system-on-chip, integrating active and passive microwave/millimeter-wave RF signal-processing components into a single chip. Design and development of CMOS millimeter-wave and microwave active and passive circuits. Field theory analysis and design of radar system engineering.

Work/Experience

Research Output/Creative Work/Innovations/Patents

- Projects & Patents:
  - Applications of Synthetic Waveguide on CMOS
  - Design and application of CMOS semi-passive inductors using tapped-inductor feedback
  - Microwave Rectenna Design
  - Design of a low-low, low-power, and high-selectivity CMOS BPF using active capacitor and feedback inductor
  - Design and Implementation of Differential DVB LNA and System Verification
  - Design and Implementation of Microwave Intruder-detection Transceiver
  - Design and Implementation of Ka-band multi-antenna transceiver

- Awards:

- Outstanding Research Award 2011, EE College, National Taipei University of Technology

- Selected Publication lists (International Journals)

[1] S. Wang, and B.-Z. Huang "Compact CMOS branch-line coupler using high-Q slow-wave transmission lines," Microwave and Optical Technology Letters, vol. 55, no. 5, pp. 1174-1178, May 2013.

[2] S. Wang, and W.-J. Lin "Design of low-power and high-gain CMOS LNA with current-reused topology," Microwave and Optical Technology Letters, vol. 55, no. 10, pp. 2429-2431, October 2013.

[3] M.-J. Chiang, S. Wang, and C.-C. Hsu, "Miniaturized Printed Slot Antenna with Multi-Ring Technique for Dual-band and Broadband Operations," IET Microwaves, Antennas & Propagation, vol. 8, Iss. 6, pp. 409-414, June 2014.

[4] S. Wang and C.-T. Chang, "K-band CMOS frequency doubler with high fundamental rejection," Electronics Letters, vol. 50, no. 17, pp. 1211-1212, Aug. 2014.

[5] S. Wang and Wen-Jie Lin, "A 10/24-GHz CMOS/IPD monopulse receiver for angle-discrimination radars," IEEE Trans. Circuits Syst. I, Reg. Papers. vol.57 no.1, pp.2999-3006, Oct. 2014.

[6] S. Wang, "A Low-Phase-Noise Ka-Band Push-Push VCO Using CMOS/GIPD Technologies," IEEE Trans. on Ultrasonics, Ferroelectrics, and Frequency Control, vol.61, no.9, pp.1456-1462, Sept. 2014.

[7] S. Wang and W.-J. Lin, "A C-band CMOS bandpass filter using active capacitance circuit," IET Microwaves, Antennas & Propagation, vol. 8, Iss. 15, pp. 1416-1422, Dec. 2014.

[8] S. Wang, M.-J. Chiang, and C-T. Chang, "A novel CMOS 24-GHz in-phase power divider using synthetic coupled lines," IEEE Trans. Components, Packaging and Manufacturing Technology, vol. 5 no.3, pp.398-403, Mar. 2015.

[9] S. Wang and C.-Y. Xiao, "Concurrent 10.5/25 GHz CMOS power amplifier with harmonics and inter-modulation products suppression," Electronics Letters, vol.51, no. 14, pp. 1058-1059, Jul. 2015.

[10] S. Wang and R.-H. Chang, "Experimental 2.4 GHz CMOS RF front-ends for non-contact vital-sign sensing," Electronics Letters, vol. 51, no. 23, pp. 1846-1848, Nov. 2015.

[11] S. Wang, and C.-C. Teng "An X-band CMOS low-noise variable amplifier with interstage reflection-type attenuator," Microwave and Optical Technology Letters, vol. 58, no. 1, pp. 196-199, January 2016.

[12] S. Wang and Po-Hung Chen, "A Low-Phase-Noise and Wide-Tuning-Range CMOS/IPD Transformer-Based VCO with High FOM T of -206.8-dBc/Hz," IEEE Trans. Components, Packaging and Manufacturing Technology, vol. 6, no. 1, pp.145-152, Jan. 2016.

[13] S. Wang and R.-H. Chang, "2.4-GHz CMOS bandpass filter using active transmission line," Electronics Letters, vol.52, no. 5, pp. 371-372, Mar. 2016.

[14] S. Wang and C.-Y. Xiao, "A 7/24-GHz CMOS VCO with High Band Ratio Using a Current-Source Switching Topology," accepted by IEEE Trans. on Ultrasonics, Ferroelectrics, and Frequency Control.

[15] S. Wang, C.-H. Lee, and Y.-B. Wu, "Fully-integrated 10-GHz Active Circulator and Quasi-Circulator using bridged-T networks in standard CMOS," accepted by IEEE Trans. on Very Large Scale Integration (VLSI) Systems.

3. Nien-Cheng Yang

Name-Last Name ..... Nien-Cheng Yang .....

Present Position ... Student .....

Education

Degree Level	Major	Institute or University	Graduation Year
M.S.	Electronics Engineering	National Taipei University of Technology, Taiwan	2018
B.S.	Electronics Engineering	National Taipei University of Technology, Taiwan	2016